NEBRASKA
Good Life. Great Journey.
DEPARTMENT OF TRANSPORTATION

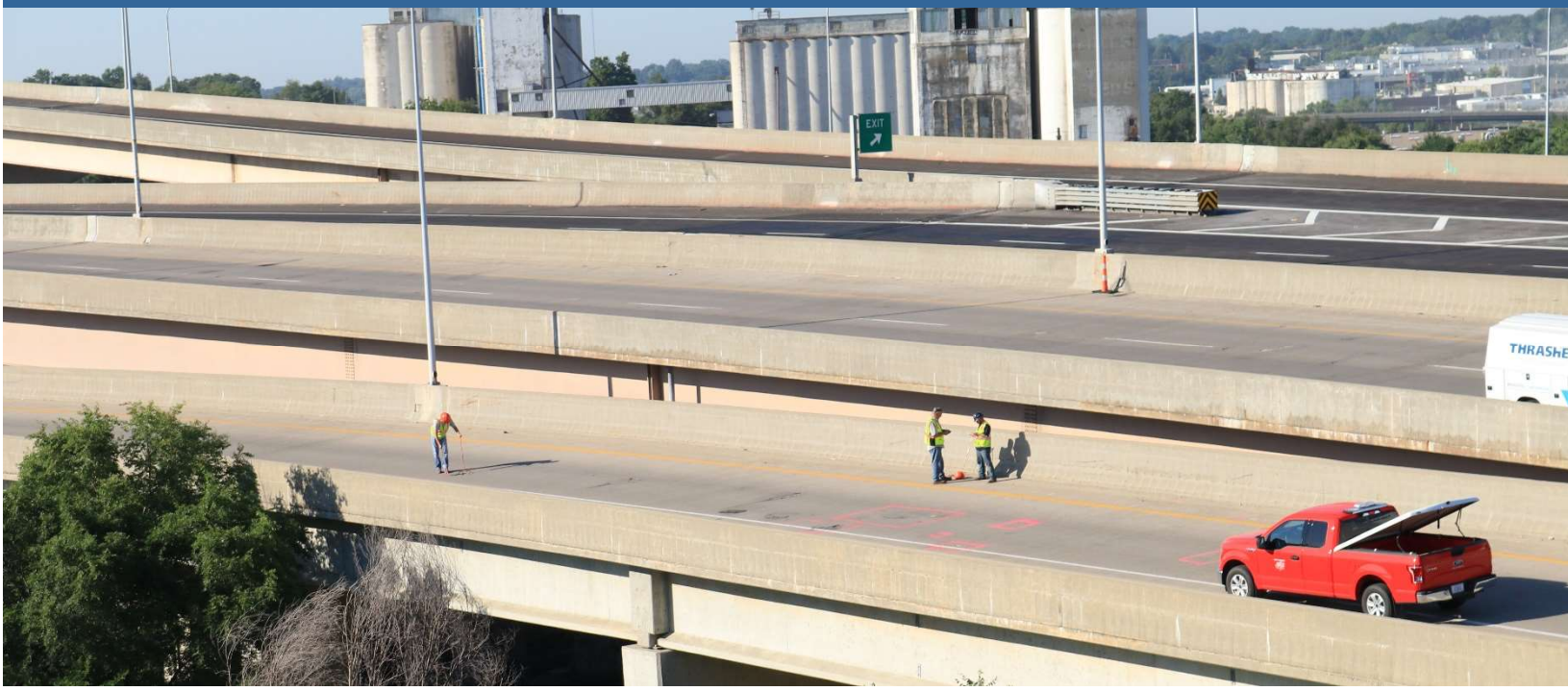

Report SPR-P1(16)M041

Automated Chain Drag Testing

Hongbin Sun, Jinying Zhu

Department of Civil Engineering
University of Nebraska-Lincoln

January 2018

Technical Report Documentation Page

1. Report No SPR-P1(16) M041	2. Government Accession No.	3. Recipient's Catalog No.	
4. Title and Subtitle Automated Chain Drag Testing		5. Report Date January 2018	
		6. Performing Organization Code	
7. Author/s Hongbin Sun, Jinying Zhu		8. Performing Organization Report No.	
9. Performing Organization Name and Address Department of Civil Engineering. University of Nebraska-Lincoln 1110 S 67th St., Omaha, NE 68182		10. Work Unit No. (TRAIS)	
		11. Contract or Grant No. SPR-P1(16) M041	
12. Sponsoring Organization Name and Address Nebraska Department of Transportation Research Section 1400 Hwy 2, Lincoln, NE 68509		13. Type of Report and Period Covered July 2015 – October 2017	
		14. Sponsoring Agency Code	
15. Supplementary Notes			
16. Abstract This report describes research work to develop an automated acoustic scanning system for rapid concrete bridge deck evaluation. The system consists of multiple channels of ball-chain impact sources and MEMs microphones for continuous acoustic wave excitation and non-contact acoustic sensing. A high precision RTK GPS with centimeter resolution provides real time positions of the scanning system. The lateral resolution is 6 inches, determined by the spacing between adjacent microphones; while the longitudinal resolution is about 1~2 inches depending on the testing speed. With a 6 feet wide testing frame (12 channels) and at a normal walking speed, it will take about 3 minutes to scan one lane of a 300 feet long bridge. Compared to link-chains used in regular chain drag test, the ball-chain impactor developed in this research show much higher sign-to-noise ratio and give very clean acoustic signals. The ball-chain gives similar impact signals as in the impact-echo test, but it can operate in a continuous excitation manner. A signal processing algorithm was then developed to map delaminations in the local coordinates of a bridge. Short time Fourier Transform (SFTF) analysis was used to extract the delamination response, which is identified as high acoustic wave amplitude in the frequency range of 0.5~5 kHz. The area and percentage of delminated bridge decks are calculated based on acoustic scanning images. The system has been validated in field tests on five bridges in Nebraska. Compared to the traditional chain drag test, the automated acoustic system significantly reduces test tine and improves accuracy. The system is ready to be deployed for routine bridge inspection.			
17. Key Words Acoustic, chain drag, bridge deck, automated.	18. Distribution Statement No restriction		
19. Security Classification (of this report) Unclassified	20. Security Classification (of this page) Unclassified	21. No. Of Pages 60	22. Price

Form DOT F 1700.7 (8-72) Reproduction of form and completed page is authorized

ABSTRACT

This report describes research work to develop an automated acoustic scanning system for rapid concrete bridge deck evaluation. The system consists of multiple channels of ball-chain impact sources and MEMs microphones for continuous acoustic wave excitation and non-contact acoustic sensing. A high precision RTK GPS with centimeter resolution provides real time positions of the scanning system. The lateral resolution is 6 inches, determined by the spacing between adjacent microphones; while the longitudinal resolution is about 1~2 inches depending on the testing speed. With a 6 feet wide testing frame (12 channels) and at a normal walking speed, it will take about 3 minutes to scan one lane of a 300 feet long bridge.

Compared to link-chains used in regular chain drag test, the ball-chain impactor developed in this research show much higher sign-to-noise ratio and give very clean acoustic signals. The ball-chain gives similar impact signals as in the impact-echo test, but it can operate in a continuous excitation manner. A signal processing algorithm was then developed to map delaminations in the local coordinates of a bridge. Short time Fourier Transform (SFTF) analysis was used to extract the delamination response, which is identified as high acoustic wave amplitude in the frequency range of 0.5~5 kHz. The area and percentage of delminated bridge decks are calculated based on acoustic scanning images.

The system has been validated in field tests on five bridges in Nebraska. Compared to the traditional chain drag test, the automated acoustic system significantly reduces test tine and improves accuracy. The system is ready to be deployed for routine bridge inspection.

DISCLAIMER

The contents of this report reflect the views of the authors who are responsible for the facts and the accuracy of the data presented herein. The contents do not necessarily reflect the official views or policies of the Nebraska Department of Roads, the Federal Highway Administration, or the University of Nebraska-Lincoln. This report does not constitute a standard, specification, or regulation. Trade or manufacturers' names, which may appear in this report, are cited only because they are considered essential to the objectives of the report. The U.S. government and the State of Nebraska do not endorse products or manufacturers.

ACKNOWLEDGMENTS

This research project would not have been possible without the funding provided by the Nebraska Department of Transportation. We would also like to thank the engineers at the Department of Transportation for their assistance in this project, and especially Mark Traynowicz, Fouad Jaber, Jason Volz, Kent Miller for providing us with the bridge information and the arrangements of traffic controls in the field testing.

Table of contents

List of figures

List of tables

1. Introduction

1.1. Introduction

Concrete bridge deck deterioration is major concern to highway agencies. Delamination is the most common type of deterioration in concrete bridge decks. The formation mechanism of delamination is complex since its occurrence is random and the pattern is irregular. Several factors may contribute to formation of delaminations in concrete. When fresh concrete is placed, the settled aggregates displace bleed water and entrapped air near the top surface, which makes the area around the water and air weaker than other parts. These weak zones will generate microcracks under loading, and then cracks develop and connect to form delaminations. Delaminations may also be caused by the corrosion of steel reinforcement (rebar). When rebar corrodes, the resulting crust expands, generates tensile stress and cracks in surrounding concrete. These cracks may create a subsurface fracture plane at the rebar level and form delaminations. The delaminations will then further accelerate severe corrosions. Although delaminations will not make structures fail immediately, the presence of delaminations may cause vertical cracks, reinforcement corrosion and spalling which will reduce the structural serviceability and lifetime.

The chain drag test is the most commonly used method for detecting delamination in bridge decks due to its low cost and ease of use [1]. It detects delaminations in bridge decks by dragging a chain over the concrete surface and listening to the hollow sound. However, this method is subjective and lack of consistency. Interpretation of test results highly depends on the experience of inspectors. Ambient noise caused by traffic also affects the test speed and accuracy of results. Since the test results are directly analyzed in the field and defects are marked on site, there is no data saved for further analysis.

1.2. Objectives

This research project aims to address the above-mentioned drawbacks of chain drag by developing an automated acoustic scanning method that integrates rapid sensing, data processing, defect identification algorithms and automated positioning in one testing system. Acoustic signals generated by the dragging chains on concrete will be sensed by acoustic sensors (microphones) and further analyzed and recorded by a computer. Including a GPS positioning system will enable real time visualization of tested areas and allow engineers to make quick assessment of bridge deck conditions. Data is saved for further analysis and for comparison with past and future tests. The proposed automated chain drag testing system will significantly improve the test consistency and speed for bridge deck evaluation, and therefore reduce the traffic disruption and bridge closure. The goal of the proposed research project is to develop an automated acoustic scanning system for rapid evaluation of concrete bridge decks. Specific objectives include:

(1) Develop an acoustic inspection device for bridge deck evaluation. Microphones are used to collect sound signals generated from the chain drag test. Replacing human ears with microphones will improve consistency of the test result interpretation, and reduce effects of ambient noises.

(2) Build a system with multiple sensor channels that is capable to cover the half or full-width lane.
(3) Integrate global positioning system (GPS) or laser positioning system to automatically track test positions and save time for documentation.

(4) Develop signal processing and defect identification algorithms, and present the test results and position information in a map view.

1.3. Report overview

This report is the product of research conducted by the Department Civil Engineering of University of Nebraska in collaboration with Nebraska Department of Transportation (NDOT). The research project focused on developing an automated acoustic scanning system for detecting delaminations in concrete bridge decks. This research project consists of six chapters. **Chapter 1** is the introduction and research objectives. Literature review related to this project is presented in **Chapter 2**. **Chapter 3** describes the acoustic testing system including sensors, data acquisition, and the comparison between the traditional steel chain and a newly developed ball-chain. **Chapter 4** presents laboratory testing on a concrete specimen. **Chapter 5** presents field testing on concrete bridge decks and a bridge deck with asphalt overlay in Nebraska. The acoustic scanning device with RTK GPS positioning system for field testing is discussed in detail. **Chapter 6** presents conclusions of this research project.

2. Literature Review

Visual inspection can only identify surface deterioration of bridge decks. In order to detect delaminations in concrete bridge decks, chain drag or hammer sounding is the most commonly used nondestructive testing (NDT) method for delamination evaluation due to its low cost and ease of use. When a chain drags over a shallow delamination, a "hollow sound" can be heard due to vibration of the delaminated concrete layer. A major drawback of the chain drag test is that it relies on subjective interpretation of the inspector, and the test is affected by the traffic noises. In addition, this method does not provide archivable data for comparison or further analysis. Ground Penetrating Radar (GPR) [2] and Infrared Thermography (IR) [3] are advanced technologies for bridge deck evaluation [4]–[6]. The two methods are usually deployed together to give a comprehensive result. However, both GPR and IR methods need expensive equipment and require special training of the operators.

Since the Impact-echo (IE) test was developed in 1980s, it has become widely used for concrete components evaluation [7], [8]. The IE test not only identifies delaminations but also gives the depth information of delamination. However, the original IE test requires physical contact between sensors/sources and concrete surface, which makes it time-consuming and labor intensive. In 2007, Zhu and Popovics [9] proposed air-coupled IE test by using a microphone to replace the contact sensor, and applied this technology to concrete bridge deck evaluation [10], [11]. Researchers have also attempted to develop automated impact sources and combine with the air-coupled sensing to increase the testing efficiency. Popovics [12] developed a non-contact scanning system for delamination detection on bridge decks. They used axle-driven impactors to generate periodical hammer impacts with impact spacing about one foot. Zhang et al. [13] used the Mel-Frequency Cepstral Coefficients (MFCC) as the delamination features and radial basis function (RBF) neural network to detect the delamination. These algorithms were incorporated into an automatic impact-based detection system. Mazzeo et al. [14] built a multichannel air-coupled scanning system with independently controlled impactors and microphones installed at each channel. This system can be towed by a vehicle and enable rapid evaluation of bridge deck conditions.

However, all these systems need complicated electrical and mechanical controls for consistent impacts, where the impact source remains a challenge for rapid scanning. On the other hand, a metal chain is a simple and effective source for continuous acoustic excitation. Combining chain drag and air-coupled sensing may provide an effective and reliable rapid scanning solution for delamination detection. University of Missisipi [16], [15] developed an automated chain dragging system that includes dragging chains, a microphone, and signal acquisition and processing components. Acoustic signals were recorded continuously and an odometer recorded the position of test. If working properly, the automated system will be more efficient and consistent than the manual chain drag test. However, this device has not been widely used in practice since it was developed in 1999. With recent development of microelectromechanical microphones, advanced signal acquisition, and GPS positioning technologies, the authors decided to revisit the chain drag

acoustic evaluation system. The purpose of this study is to address deficiencies in the current chain drag scanning system and develop a rapid and reliable acoustic scanning system.

Figure 2-1 Automated Chain Drag System [15]

3. Acoustic Scanning System

The developed acoustic scanning system includes the following components: excitation source (steel chain or ball-chain), acoustic sensors (microphones), data acquisition (DAQ), and positioning devices. The acoustic sensor and sources are described in detail below, and the positioning device is described in field testing section.

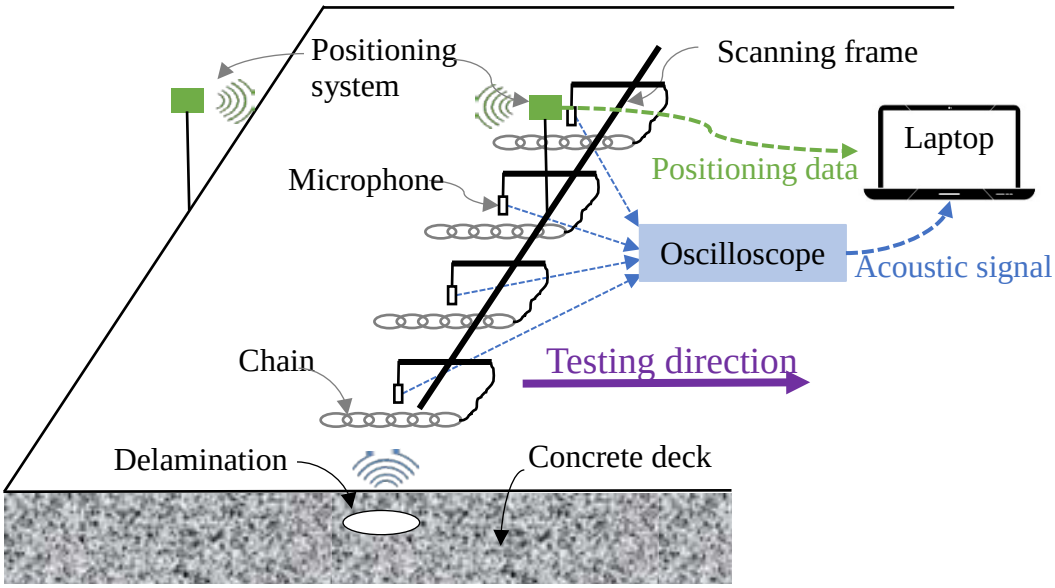

Figure 3-1 Schematic diagram of automated acoustic scanning system

3.1. Acoustic sensor and data acquisition

Previous studies [9]–[12], [16] have successfully used microphones as acoustic sensors for detection of delaminations in bridge decks. The application of MEMS (microelectro-mechanical systems) technology to microphones has led to the development of small microphones with very high performance. MEMs microphones have much smaller size and very low cost (less than $1 each) compared to regular microphones. In this study, analog MEMS microphone (Adafruit SPW2430, see **Figure 3-2**(a)) with a frequency range of 100 Hz to 20 kHz were used as acoustic sensors. This MEMS microphone needs a 3.3-5 V DC power supply. The measured sensitivity is about 12.9 mv/Pa. Detailed parameters of the MEMS microphone are shown in Appendix A.

The automated chain drag system developed by University of Mississippi used only one microphone to sense the acoustic energy by multiple chains. This design may give low lateral resolution that depends on the total width of all chains. In order to improve the lateral spatial resolution, we used a multi-channel sensing system, which provided wide lateral coverage with good spatial resolution. Each channel includes a MEMs microphone and a steel chain installed right beneath the microphone. As shown in **Figure 3-1**, multiple MEMs microphones and chains are installed on a testing frame at equal lateral spacing about 4 to 6 inches. The spacing determines

the lateral spatial resolution of acoustic scanning. The acoustic signals excited by each chain will be sensed by the corresponding microphone, and then digitized by a multi-channel data acquisition device. For example, a system with 12 microphones at 6 inch spacing will give a lateral coverage of 6 feet In laboratory studies, an 8 channel oscilloscope (PICO 4824, see **Figure 3-2**(b)) with a sampling rate of 100 kHz was used. A LabVIEW program is developed to control data acquisition and display the time domain signals, positioning data during scanning. A two-dimensional image would be generated after scanning.

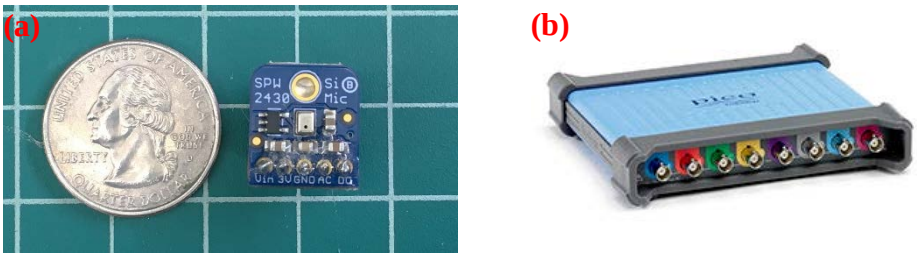

Figure 3-2 System components: (a) MEMS microphone; (b) PICO scope 4824

3.2. Acoustic sources

3.2.1. Steel link chains and ball-chains

Steel link chains were initially used in the study. Due to high noise level caused by these chains, we later developed a new ball chain impact source. To differentiate the conventional chains used in the chain drag test and the newly developed ball- chain impactor, we denote the conventional chain as “steel chain”, while call the new source as “ball-chain”. Both types of chains were tested on solid concrete surfaces and delaminations to evaluate their performance for defect detection and signal to noise ratio (S/N).

Many types of link chains are available, and they vary from material, coating, length per segment and weight. We tested ten different types of link chains (see **Figure 3-3**) and investigated noises caused by link clapping in air and surface friction when dragging on concrete surface. Test results indicate all links chains created high level noise in air, and many also have high level of noise when dragging on solid concrete surface. We chose link chains C5 (chain 1), C7 (chain 2) and the ball chain for detailed discussion. **Figure 3-4** shows two different types of steel link chains and the newly developed ball-chain.

Both steel chains have the same ¼-in diameter but with different surface finishing. Chain 1 has a shinny zinc-plated surface, while chain 2 has a galvanic surface finishing. The ball-chain consists of two ½-in and two 5/8-in brass balls connected by a flexible nylon string. The distance between the first and last ball is about 4 inches. Using different sizes of balls allows different impact contact times, which is useful to identify delaminations with different resonance frequencies. A smaller ball is more effective for delaminations with higher frequency and a larger ball is for delaminations with lower frequency.

Figure 3-3 Ten different types of steel link chains

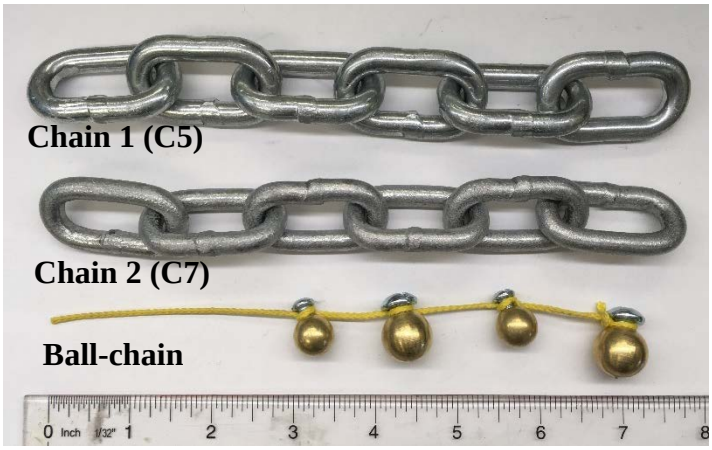

Figure 3-4 Two steel chains and a ball-chain

3.2.2. Signal processing

When a chain drags on concrete surface, a microphone and the DAQ continuously record acoustic signals in steam mode. Because delamination response is easy to identify in frequency domain, the continuous time domain signals were processed using Short Time Fourier Transform (STFT). The STFT procedure divides a long time signal into many short segments of equal length (N samples) and then compute the Fourier transform separately on each short segment. A 2-D image called STFT spectrograms is then generated by plotting amplitude spectra for all segments, with the x-axis as the signal time and y-axis as the frequency. The color scale in the 2D image represents the amplitude of frequency spectra. Therefore, STFT is able to show signal frequency content change over time.

3.2.3. Noise in air

It was noticed that a high level noise around 15 kHz presented in most chain drag tests. It is assumed this noise might be caused by the clapping between links. In order to verify this assumption, a chain was shaken in air and a signal of one-second duration was collected. The time domain signal and the STFT spectrogram are shown in ***Figure 3-5***. This result confirms that the high level acoustic energy around 15 kHz was caused by link clapping of chains.

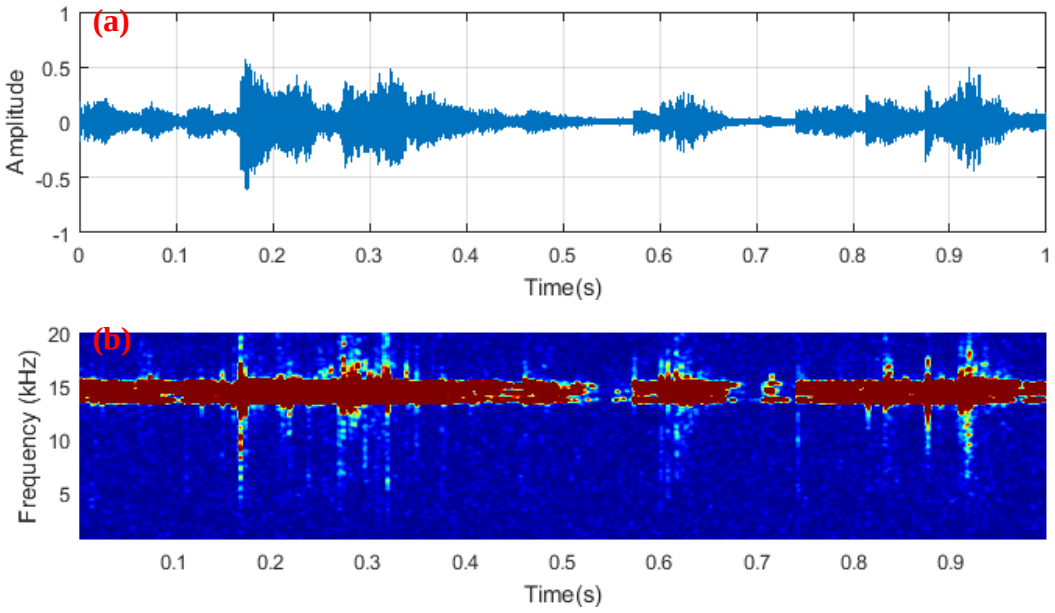

Figure 3-5 Chain 1 vibrating in air: (a) Time domain signal; (b) STFT image

3.2.4. Chain drag test on solid concrete surface

When a chain drags over concrete surface, delaminations in concrete tend to give higher level acoustic responses than the solid region. Therefore, an ideal acoustic source should have low acoustic energy in the frequency range of interests. According to a semi-analytical analysis of resonance frequencies for square concrete delaminations by Kee and Gucunski [17], the resonance frequency ranges from 0.5 to 5 kHz for delaminations with a depth of 20~80 mm (0.8~3.2 inches) and width of 0.2 m ~1 m (8~ 40 inches). Therefore, the major criterion for selecting proper excitation sources is to ensure low noise level in 0.5~5 kHz frequency range in solid concrete regions.

Acoustic signals were collected by dragging chain 1, chain 2 and the ball-chain on a solid concrete surface. The time domain signals and STFT spectrograms are shown in ***Figure 3-6***. Both link chains show high level noise around 15 kHz (see **(b)** and **(d))** when dragging on solid area. As discussed previously, the 15 kHz noises came from the clapping between chain links (**Figure 3-5**).

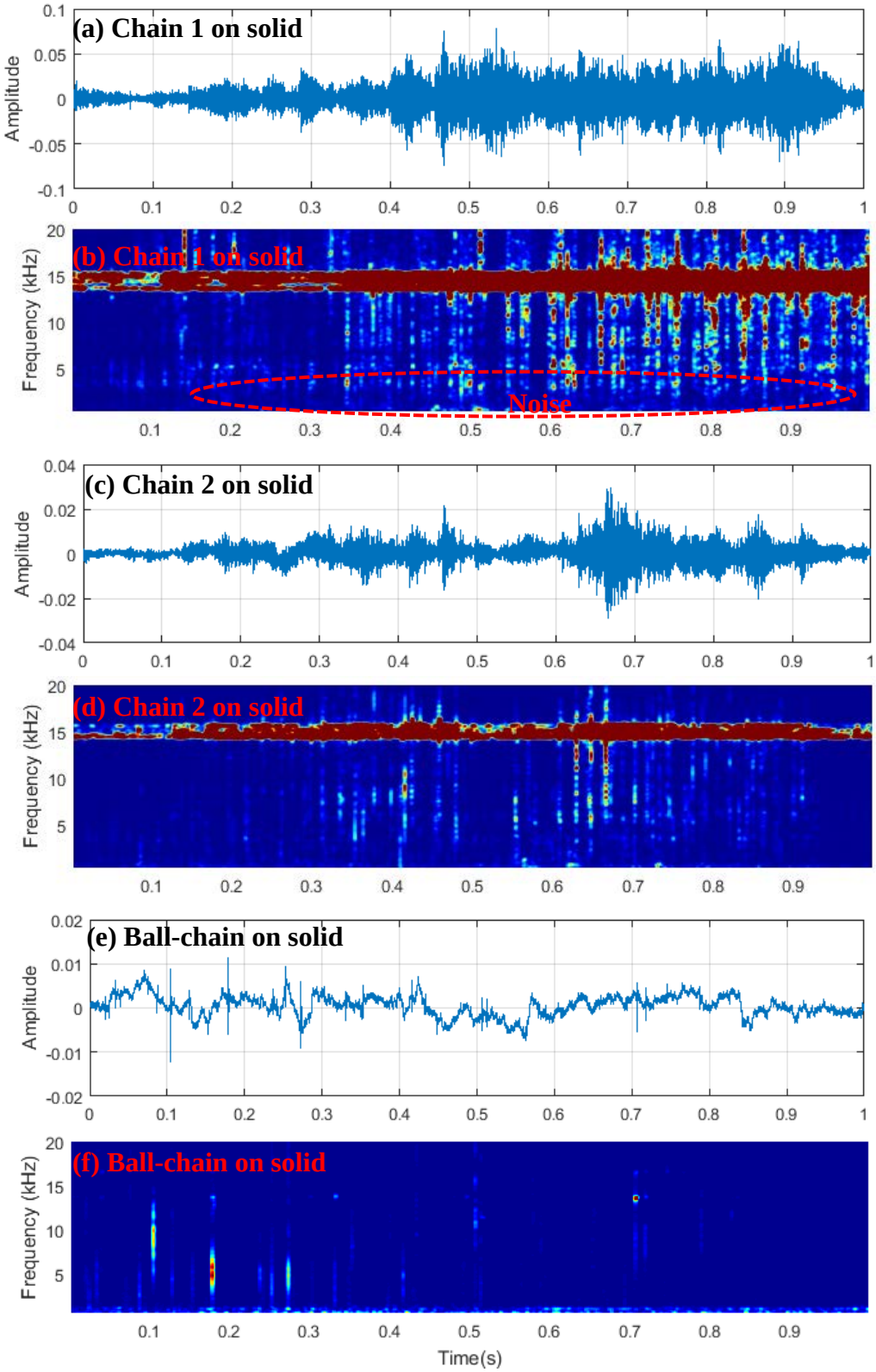

Figure 3-6 Time domain signals and STFT spectrograms of chain dragging on solid concrete surface

For shallow delaminations, the resonance modes are dominated by flexural vibrations. Unlike the impact-echo mode, the flexural vibration resonance frequencies depend on the depth, lateral dimensions and boundary conditions of delaminations. Kee and Gucunski [17] derived the semi-analytical equation of resonance frequencies for square delaminations:

$$f_1 = \varepsilon\beta_2 \frac{C_p}{h}\left(\frac{h}{c}\right)^2 \qquad 3\text{-}1$$

where

$$\beta_2 = \frac{\pi\sqrt{(1-2\upsilon)}}{\sqrt{12(1-\upsilon)^2}},\ \epsilon = 1.64e^{0.0014(h/c)} - 1.81e^{-0.22\left(\frac{h}{c}\right)} \qquad 3\text{-}2$$

in which C_p is the P-wave velocity of concrete, υ is the Poisson's ratio of concrete, h is the depth of the delamination and c is the width of the delamination. In this experiment, the P-wave velocity is 4400 m/s and the Poisson's ratio is 0.22. Base on the two equations, relationships between frequency and delamination width are plotted in **Figure 3-7** for two depths: 1 inch and 3 inches. For depth of 1 inch, delaminations with width of 4.9 to 30 inches have the first three resonant frequencies in the range of 0.5 to 5 kHz. For depth of 3 inches, the width range is from 5 inches to 50 inches. It can be seen that the frequency range 0.5 to 5 kHz will cover major resonance modes for delaminations with lateral dimension in the range of 5-30 inches and at depth of 1-3 inches. In practice, most bridge deck delaminations occur at the top layer rebars, with a depth of 1-3 inches. Therefore, the major criterion for selecting proper sources is to ensure low noise level in 0.5 kHz to 5 kHz frequency range.

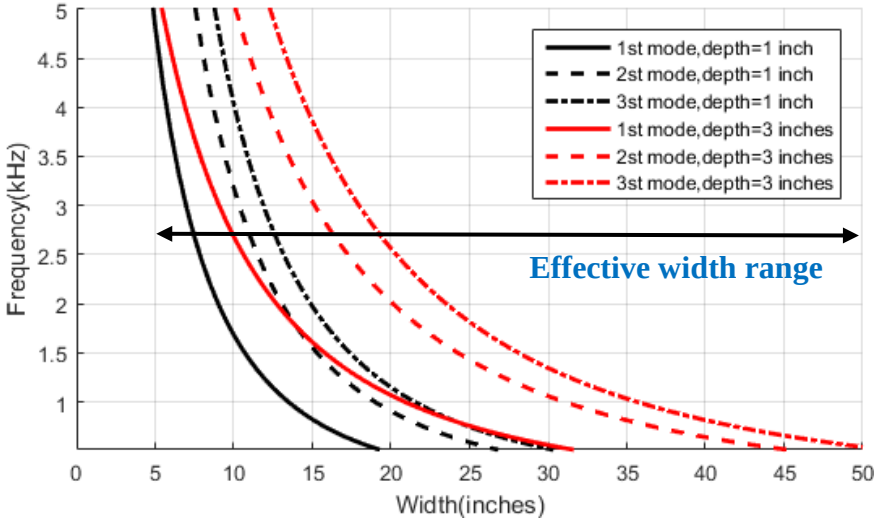

Figure 3-7 Relationships between resonance frequency and delamination width

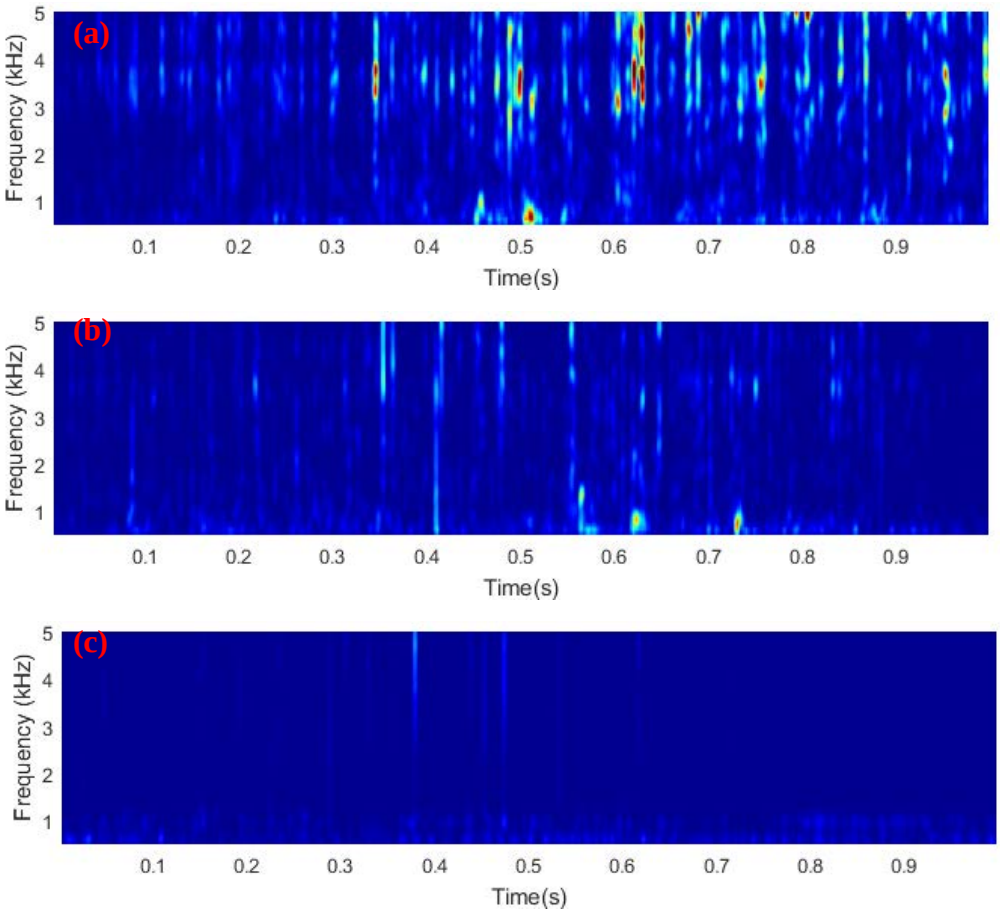

Figure 3-8 STFT images (0.5-5kHz) of signals on solid concrete surface by dragging (a) Chain 1; (b) Chain 2; (c) Ball-chain

Figure 3-8 presents the STFT spectrograms of chain 1, chain 2 and ball-chain signals in the frequency range of 0.5~5 kHz. It is clear that chain 1 generated more noises than chain 2 and the ball-chain. Other chains investigated in this study showed the similar problem. These noises will contaminate the delamination resonance signals and may give false positive indication of delamination. Chain 2 and the ball-chain present cleaner signals. The rough surface finishing of chain 2 may attribute to the low noise level. In studies presented in the following sections, chain 2 and the ball-chain were used for further testing on the concrete specimen in laboratory.

4. Acoustic Testing on Laboratory Specimen

4.1. Specimen design for laboratory testing

A 10 feet by 4 feet reinforced concrete slab (4 inches thickness) was fabricated with four artificial delaminations of different sizes and depths (see **Figure 4-1**). A polymethyl methacrylate sheet covered with black plastic film was used to create an artificial delamination. The slab was cast with ready mixed self-consolidated concrete (SCC). Sizes and depth of four delaminations are marked in the figure below**.**

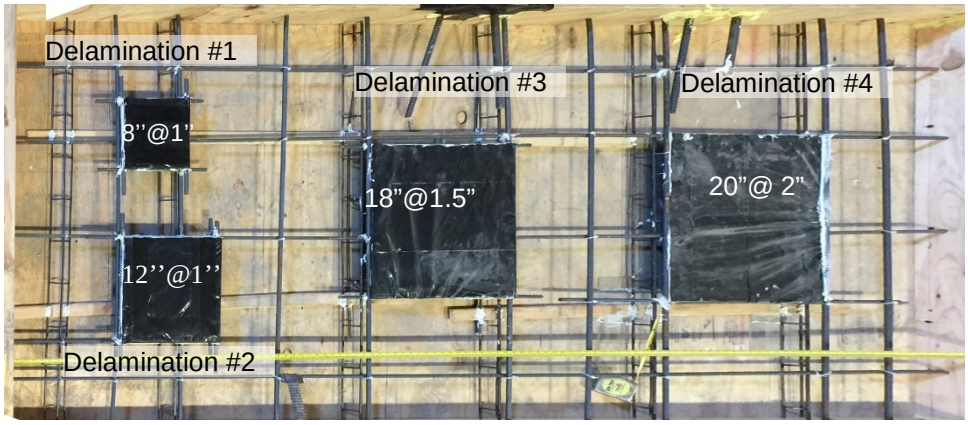

Figure 4-1 Concrete specimen with four artificial delaminations

4.2. Resonance frequencies of delaminations

Before performing the chain drag test, we used impact-echo test to measure the flexural mode resonance frequencies of the four delaminations using an accelerometer. The impacts were applied at the center of DL1 and DL2, and at the edge of DL3 and DL4. It was easy to hear hallow sound when a steel ball tapped on these regions. The time domain signals and their frequency spectra are shown in **Figure 4-2**. The resonance frequencies are summarized in **Table 4-1**. Only frequencies below 5 kHz are shown.

Table 4-1 Dimensions and resonance frequencies of four delaminations

Delamination	Size	Depth	Resonant frequency		
			1st	2nd	3rd
DL1	8 x 8''	1''	2.9 kHz	--	--
DL2	12 x 12''	1''	1.7 kHz	3.1 kHz	--
DL3	18 x 18''	1.5''	0.75 kHz	1.4 kHz	2.3kHz
DL4	20 x 20''	2''	0.7 kHz	1.4 kHz	2.6 kHz

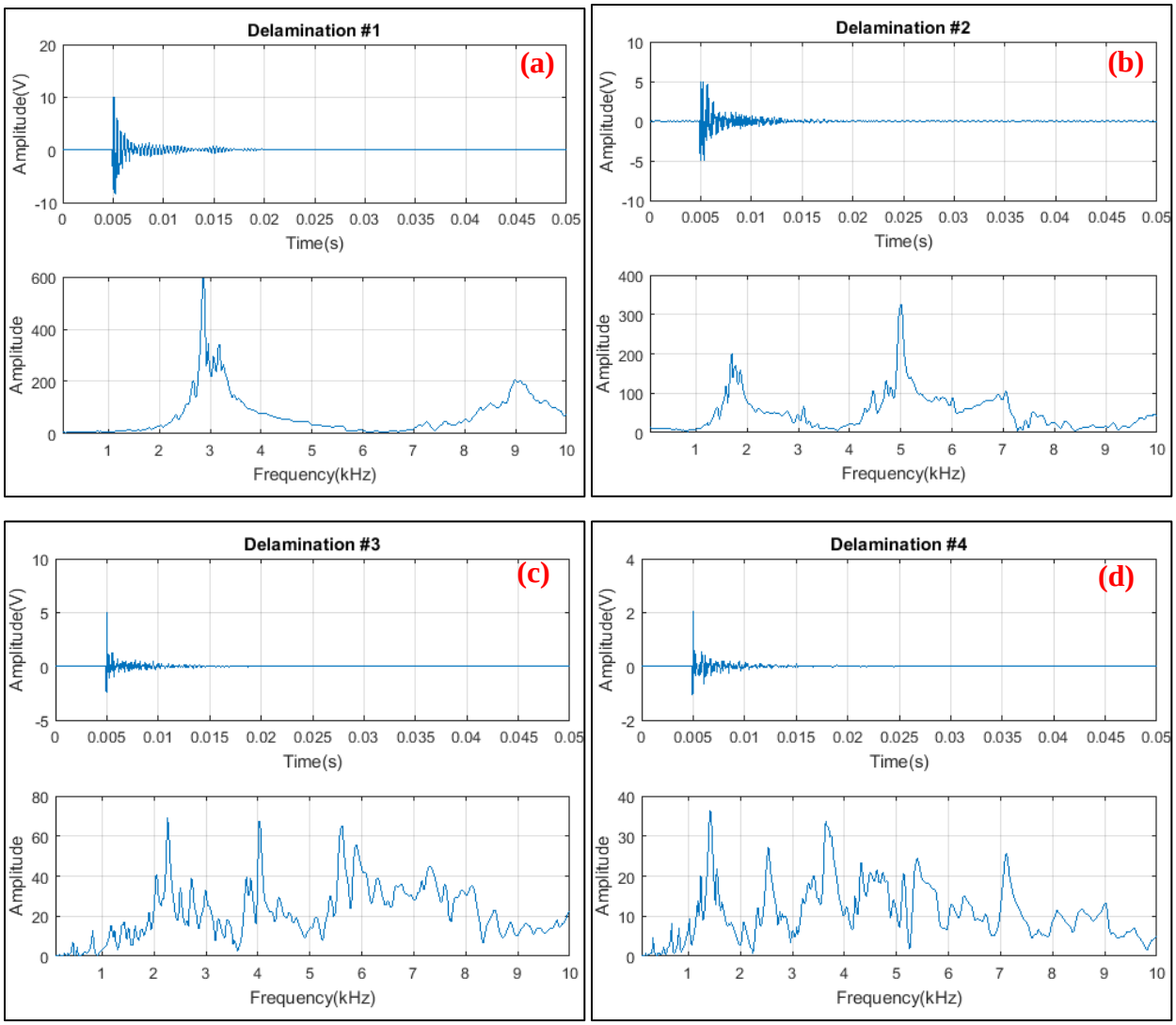

Figure 4-2 Time domain signals and frequency spectra on delaminations: (a) #1; (b) #2; (c) #3; (d) #4. A steel ball impactor and a contact accelerometer were used in the test.

4.3. Scanning system for the laboratory specimen

A scanning system was designed for testing on the concrete slab. Two aluminum rails were installed along the longer sides of the concrete slab, and a horizontal frame supported by the rails can move in the longitudinal direction. Six microphones were installed along the sliding frame at equal spacing, and six chains (link chain or ball chain) were installed right under each microphone as acoustic source. A laser distance sensor (SICK Dx35, SICK AG.) was used to measure the positions of the sliding frame in real time. The sensor provides analog output voltage proportional to the distance. The laser sensor was installed at the one end of the specimen and a reflective tape was installed on the sliding frame. All six microphones and the laser sensor were connected to the PICO scope for data acquisation.

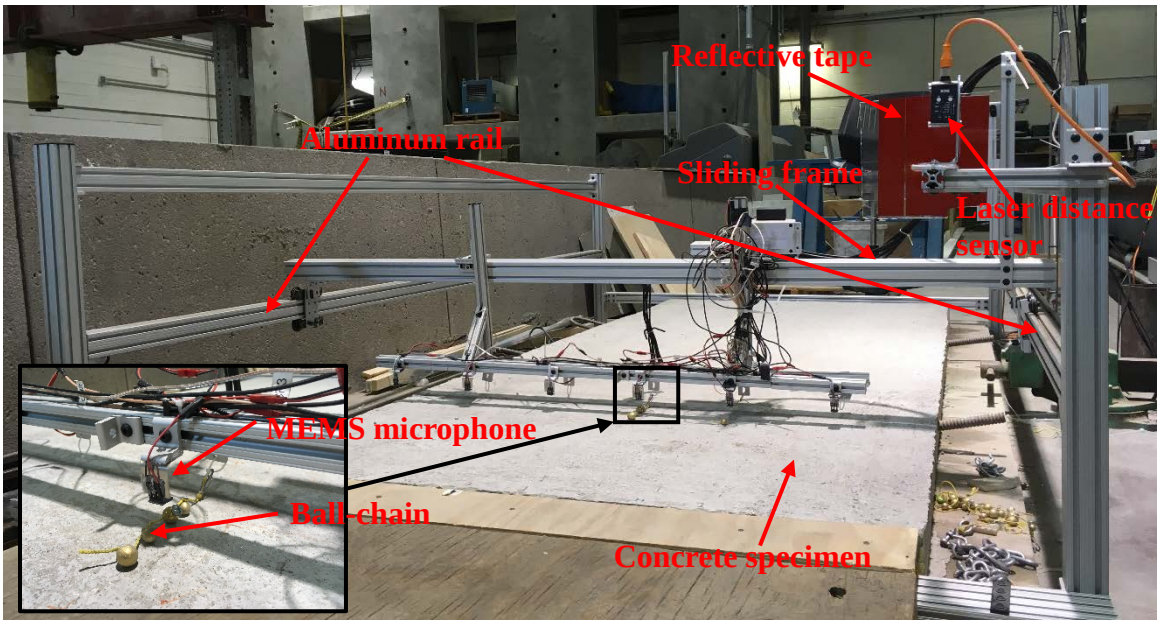

Figure 4-3 Scanning frame for concrete slab

4.4. Steel link chain and ball-chain testing on delaminations

The delaminations were scanned along their centerlines using Chain 2 and the ball-chain, respectively. The time signals were first processed by STFT to generate spectrograms. Because the laser distance sensor was synchronized with the acoustic signals, the time axis of each spectrogram can be converted to distance using the distance sensor data. The distance was measured from the left edge of the specimen (**Figure 4-1**). The distance based spectrograms of scanning signals on the four delaminations (DL1, DL2, DL3 and DL4) are shown in **Figure 4-4**. The link-chain results are shown in the left column, while the ball chain results are shown in thr right column. Delamination resonance frequencies are highlighted with white rectangles, and the peak frequency values are marked. The actual boundaries of the delaminations are represented by the vertical lines in the spectrograms.

Both the link-chain and the ball-chain were able to detect DL1 and DL2 clearly. For DL1, only the the first resonance mode was shown; for DL2, the first two resonance modes are identified, and the frequencies match the impact echo results shown in **Table 4-1**. Delamination #3 is deeper than delaminations #1 and #2 (1.5 inch vs. 1 inch), and therefore the acoustic response is weaker due to increased flexural stiffness with depth. Although both Chain 2 and the ball-chain detected the third resonance frequency well, the Chain 2 image has much more noise. Delamination #4 was proven very challenging for manual chain drag by human hearing. Chain 2 could excite the second resonance mode clearly, but the first mode excitation is inconclusive due to high level noise. As comparison, the ball-chain result clearly shows 4 resonance modes with very clean background.

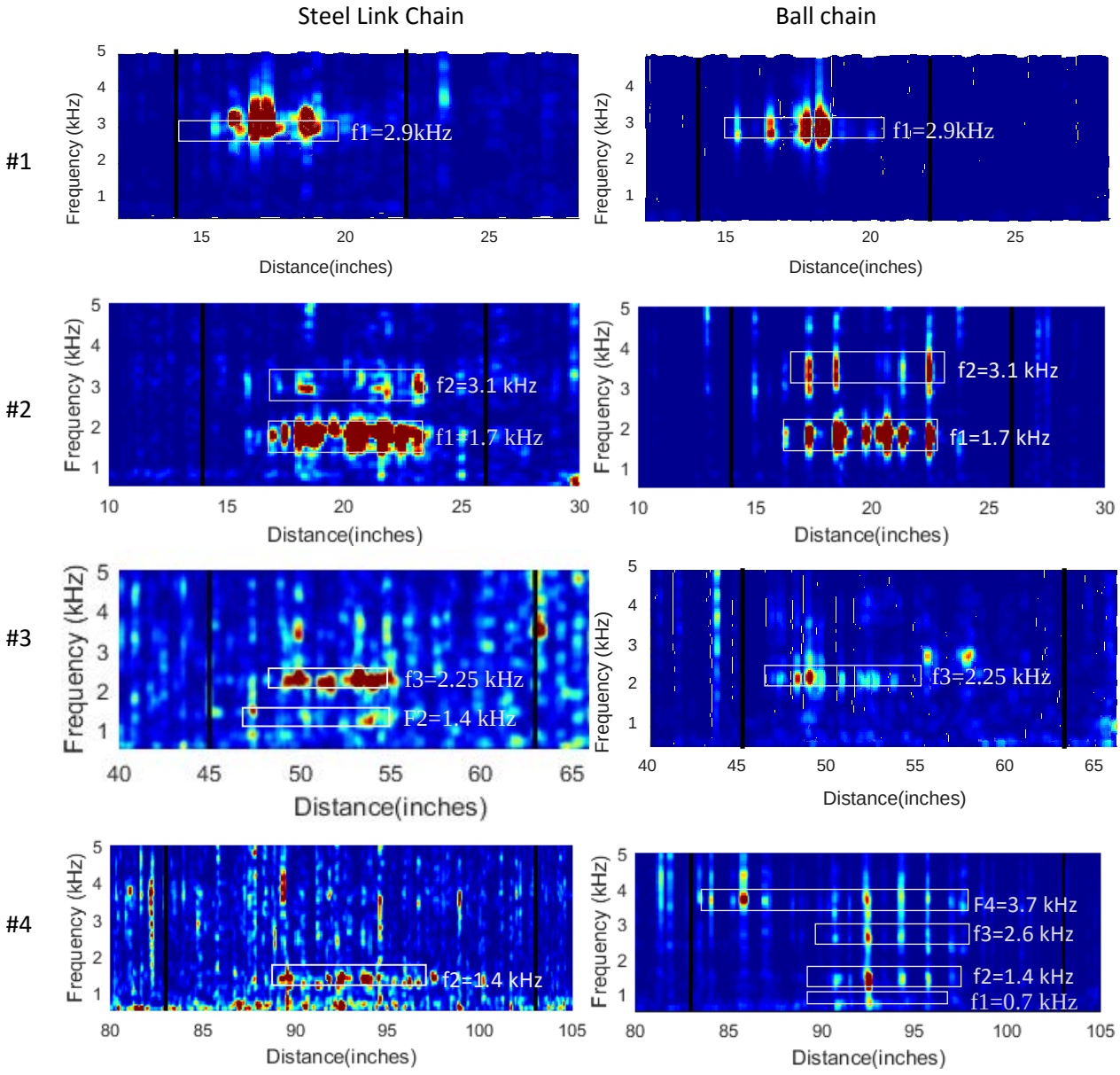

Figure 4-4 STFT spectrograms of signals by dragging a steel link chain (left column) and a ball-chain (right column) on four delaminations.

4.5. Impact mechanisms of link chain and ball-chain

By comparing the spectrograms shown in **Figure 4-4**, it is easy to draw conclusions that the ball chain gives much cleaner signals. For the ball chain, acoustic energy is only generated by the impacts of the balls on the concrete surface; for the link chain, noise is also generated by link clapping and surface friction, which contribute little to vibration of delamination. Furthermore, visual inspection shows that the concrete surface is very rough, and broadband noise is generated from the friction between chain and surface.

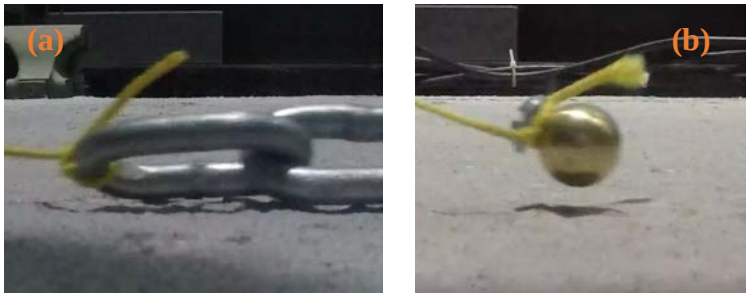

Figure 4-5 (a) Chain sliding on slab; (b) Ball jumping on slab

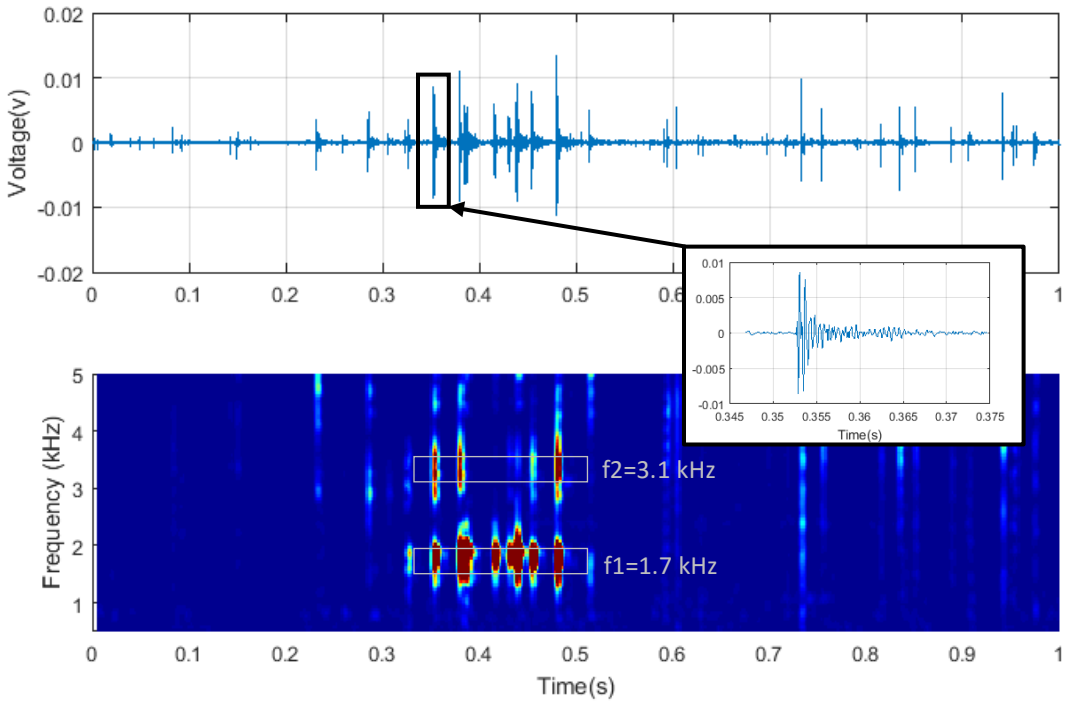

Figure 4-6 Time domain signal and STFT image of ball-chain dragging on delamination #2

We used slow motion videos to investigate the behavior of steel link-chain and ball chain when they were dragged on concrete surface. A GoPro camera was used to capture footages of dragging both chains on concrete surface at a frame rate of 240 frames per second (fps), then videos were played at a frame rate of 10 fps (1/24 original speed). In the slow-motion videos, it can be found that the link-chain mainly slid on the concrete surface, while the ball-chain jumped and impacted on the concrete surface periodically (see **Figure 4-5**). The jump-and-impact behavior is similar to the impacts in a continuous impact-echo test, which gives high S/N in the acoustic signals.

Figure 4-6 presents a time domain signal and its STFT spectrogram when the ball-chain was dragged over DL2. In the time domain signal, multiple high amplitude spikes represent ball impacts on the concrete surface and each spike (see the inset) is a typical impact-echo test signal These spikes correspond to the vertical bright strips in the STFT spectrogram. The high amplitude resonance response (red spots) of DL2 occurs around its resonance frequencies (f1 = 1.7 kHz and f2 = 3.1 kHz) that match the impact-echo test results well.

4.6. Scanning image of the entire concrete slab

Both the link-chain and ball-chain were used to scan the entire concrete specimen. Six channels with an 8-inch spacing was used to cover the 48-inch wide concrete slab. In order to improve the lateral spatial resolution, the chain/sensor locations were shifted by 50mm in lateral direction in each scan, and three more shifted scans were performed, as shown in **Figure 4-7**. In total 24 scanning signals were recorded in each test.

A 2D acoustic scanning image of the specimen will be built using the collected 24 signals. The longitudinal dimension will be obtained by converting the signal time to distance using the distance sensor data, while the lateral dimension is represented by the position of each channel. Since each signal represents a 1D scan along a line in the longitudinal direction, its 2D spectrogram should be compressed to 1D format. In order to keep energy invariance during signal conversion, we define the signal energy **S** at each STFT time segment (or distance) using the following formula, i.e. integrating the power spectrum over the frequency range of 0.5~5 kHz.

$$S = \int_{0.5}^{5} |X(f)|^2 \, df \qquad 4.1$$

where $|X(f)|^2$ is the signal power spectrum obtained from STFT and df is the frequency spacing. The symbol S represents the energy contained in the acoustic signal within the bandwidth of 0.5 ~5 kHz. If the microphone output signal has a unit of Volt (V), then S has a unit of V^2.

A one-dimensional signal energy **S** vs. scanning distance is then formed for each scanning signal. Since the signal energy **S** is a very small value, it is convenient to express it in decibel (dB) by taking the background signal energy level $\mathbf{S_b}$ as the reference. Our experimental data indicate that the $10\log S_b$ is about -55 for signals in solid regions. Therefore, we define the relative energy **S(dB)**

$$S(dB) = 10\log\frac{S}{S_b} = 10\log S - 55 \qquad 4.2$$

By stacking the **S(dB)** data sets from all channels, a two-dimensional map is generated, with two axes representing distance in the longitudinal (scanning) and transverse (across channels) directions. The amplitude of each pixel in the 2-D map represents the signal energy level **S(dB)** in the frequency range 0.5~5 kHz.

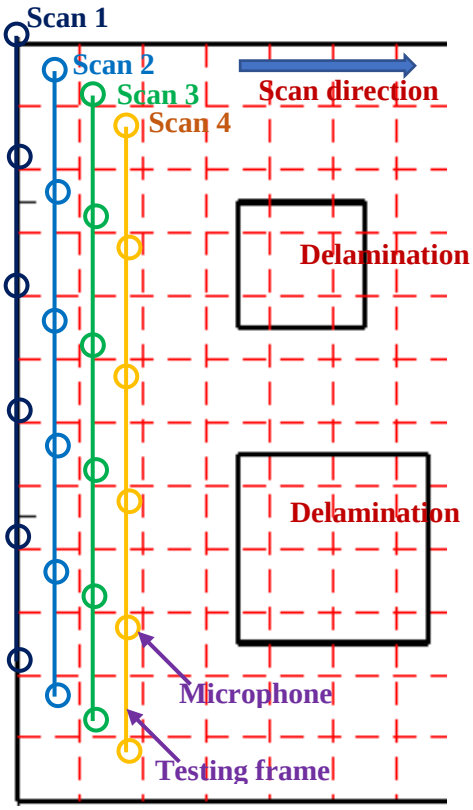

Figure 4-7 Schematic diagram of slab full scanning

Figure 4-8 shows the scanning images using the link chain and the ball-chain. Both images use the same color scale 5-10dB, where blue color represents low signal energy in the frequency range 0.5~5 kHz, and red color represents high signal energy level. Generally, shallow delaminations will give high acoustic signal energy levels. In this study, both the steel link-chains and the ball-chains detected DL1 and DL2 clearly. In the link-chain image, however, many false positives present in the solid area around DL3 due to very rough surface in this region, while the ball-chain image shows more accurate results for DL3. Detailed analysis indicates that the bright spots in DL4 could be caused by rough surface noise instead of delamination responses. However, in the ball-chain image, DL4 can still be identified although the delamination response is much weaker than other delaminations. It can be concluded that the ball-chain gives higher S/N and is less susceptible to effect of surface roughness. It should be noted that the artificial delaminations appear

more rigid than actual delaminations in bridge decks. Experience indicates that actual delaminations with similar dimensions as DL4 (50×50×5 cm3) can be detected by the chain drag test. Based on these results, we decided to use the ball-chain as the excitation source to design a scanning cart for field test.

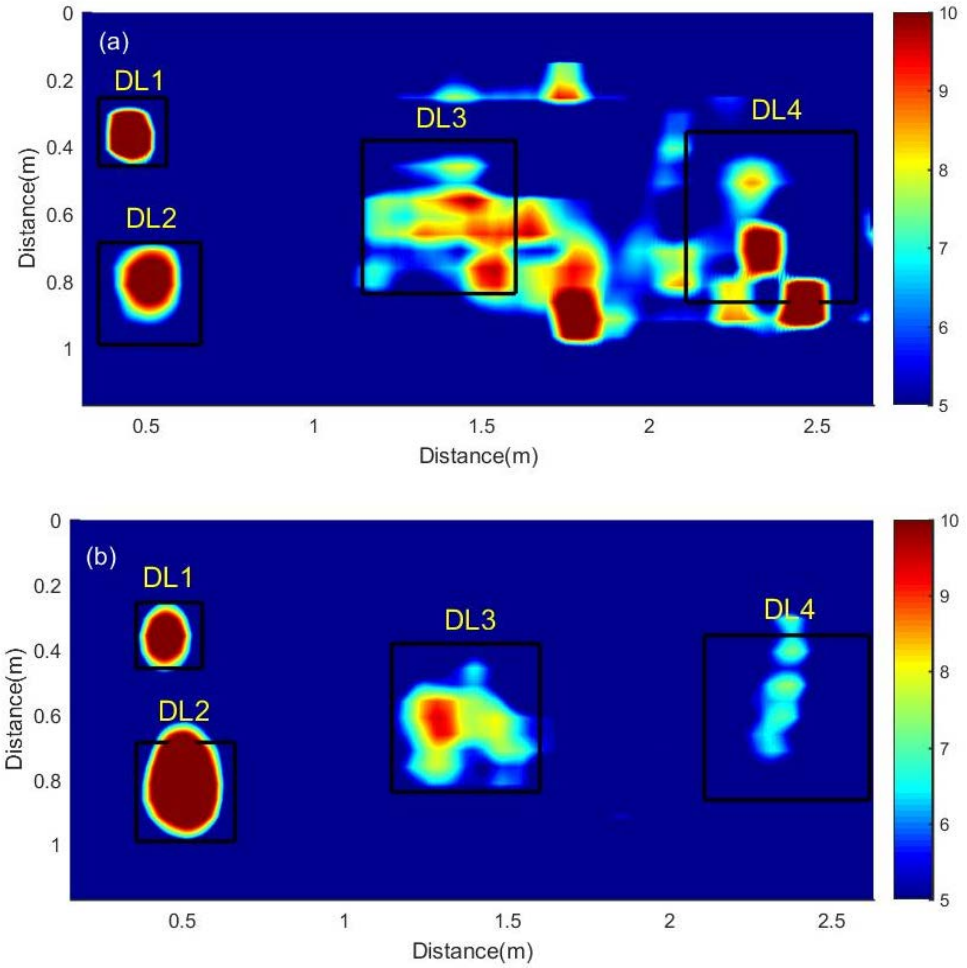

Figure 4-8 Full scanning images using (a) Chain 2, (b) Ball-chain

4.7. Scanning speed effect

Moving speed will affect testing results on two aspects: spatial resolution and impact energy level. Spatial resolution is defined by the distance between two adjacent impacts. Increasing ball-chain dragging speed will increase the ball impact energy on concrete surface and amplitude of acoustic signals, but it may lead to poor spatial resolution due to large spacing between two impacts. In this study, a ½ inch diameter brass ball was dragged on the concrete surface at four different speeds (10 in/s, 20 in/s, 30 in/s, 40 in/s). Each signal was processed by STFT and the spectrograms are shown in **Figure 4-9**. Each high amplitude (red) vertical strip in the image represents an impact on the surface. At a low dragging speed, more impacts are observed in a given unit length. A higher test speed produces fewer impacts in the same length. The spatial resolution is calculated as the total dragging length divided by the number of impacts. There are 22, 14.4, 9.3 and 4.2 impacts

per meter (spatial resolution: 0.54 inches, 0.83 inches, 1.28 inches, 2.8inches) for the scanning speeds of 10 inches/s, 20 inches/s, 30 inches/s, 40 inches/s respectively. The peak voltage of each impact signal was measured and converted to sound pressure level (SPL) using the microphone's sensitivity (12.9 mv/Pa). The average SPLs at the four dragging speeds were 83.6 dB, 87.4 dB, 91.4dB and 97.5 dB. The spatial resolution and sound pressure level are summarized in **Table 4-2**. It is seen that a higher scanning speed leads to higher energy for each impact, but it gives lower spatial resolution (larger spacing). Therefore, there is a tradeoff among testing speed, spatial resolution, and signal amplitude. Based on our experience, a speed of 20~30 in/s provides a good balance of spatial resolution and impact energy.

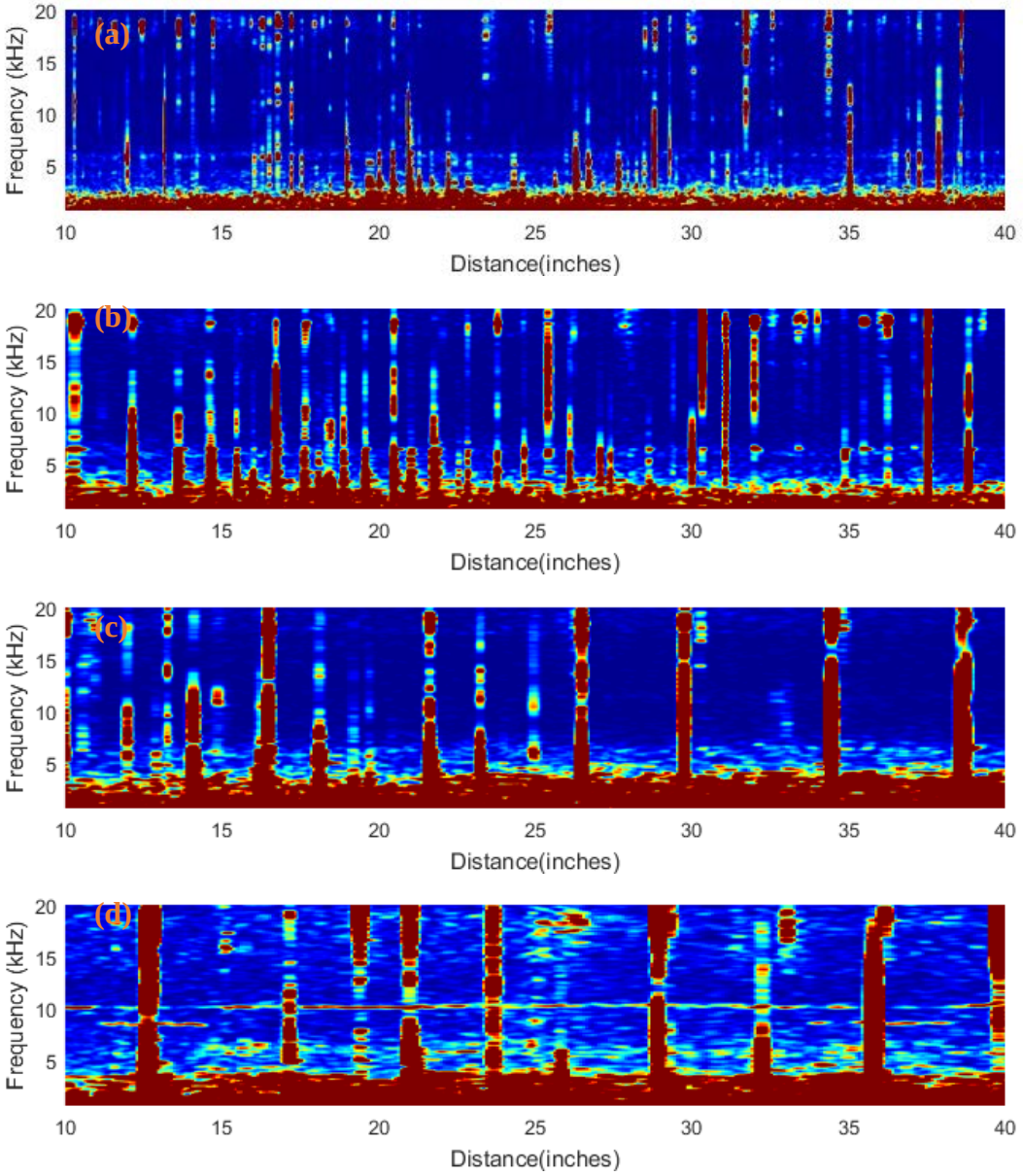

Figure 4-9 STFT images of four test speeds: (a) 10 in/s, (b) 20 in/s, (c) 30 in/s, (d) 40 in/s

Table 4-2 Spatial resolution and sound pressure level of four dragging speed

Speed (inches/s)	Spatial resolution (inch)	Sound pressure level (dB)
10	0.54	83.6
20	0.83	87.4
30	1.28	91.4
40	2.4	97.5

4.8. Increasing spatial resolution using multiple balls

In order to improve testing speed and signal amplitude without scarifying the spatial resolution, we connected multiple balls in parallel as the excitation source (**Figure 4-10**). Each ball will impact the concrete surface randomly and independently. This design increases the total number of impacts per unit length. The time domain signals of using different numbers of balls are shown in **Figure 4-11**. When increasing the number of balls, the time domain signals show more spikes which means more impacts and smaller spatial spacing. At a speed of 33 in/s (0.86m/s), the spatial resolutions are 1.7 in, 1.1 in, 0.9 in and 0.7 in when using 1, 2, 3 and 4 balls respectively. It is found that the spatial resolution does not increase linearly with the number of balls. Since the ball size affects frequency content of impact, we combined two small size balls and two large size balls (such as two ½ in balls and two 5/8 in balls) to cover delaminations with different fundamental frequencies.

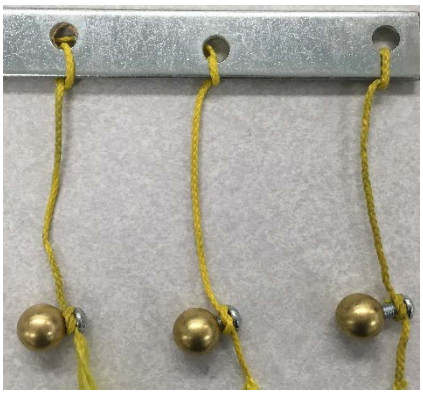

Figure 4-10 Three parallel metal balls as excitation source

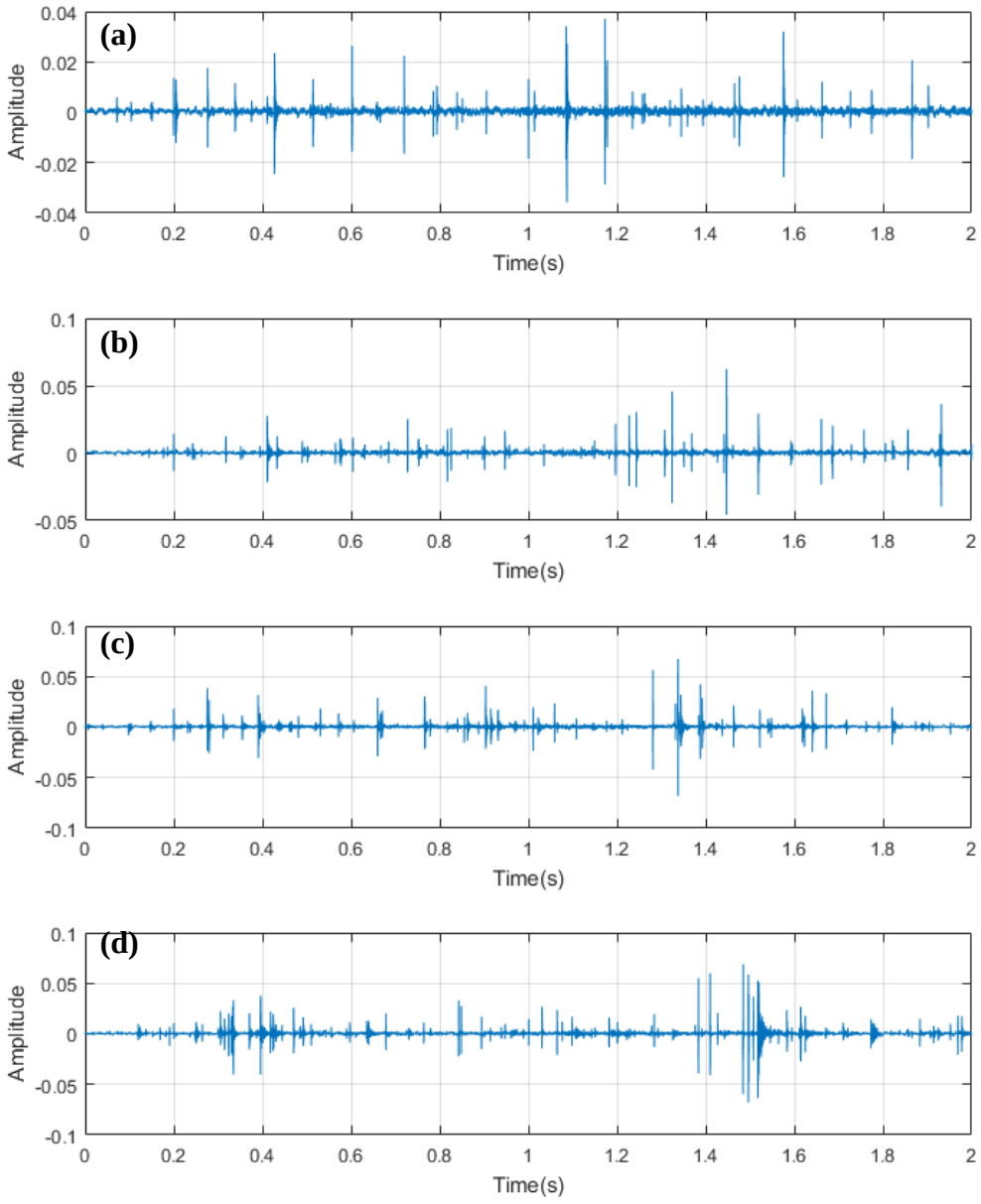

Figure 4-11 Time domain signals of : (a) one ball; (b) two balls; (c) three balls; (d) four balls

5. Field Testing on Concrete Bridge Decks

5.1. Scanning cart design

A scanning cart with 8 channels of microphones was designed for field test, as shown in **Figure 5-1**. A microphone array was installed on a 6-ft wide frame with a spacing of 6 inches, and connected to an oscilloscope mounted on the cart. Data from the oscilloscope will be transferred to laptop computer with a LabVIEW program, and a final scanning image with positioning information will be generated when scanning is finished. During the scanning, a GoPro camera will record the surface condition at the same time. The videos will be used to check the surface condition of bridge deck.

A Real Time Kinematic (RTK) GPS (Piksi GPS, Swift Navigation, Inc.) was used to provide real-time positions of the scanning cart (see **Figure 5-2**). The RTK GPS has two same modules, with one module fixed as the base station and the other installed on the moving cart as a rover. The two GPS modules will communicate with each other using 900MHz radio to get RTK fix, a high accuracy GPS data. The GPS working diagram is shown in **Figure 5-3**.

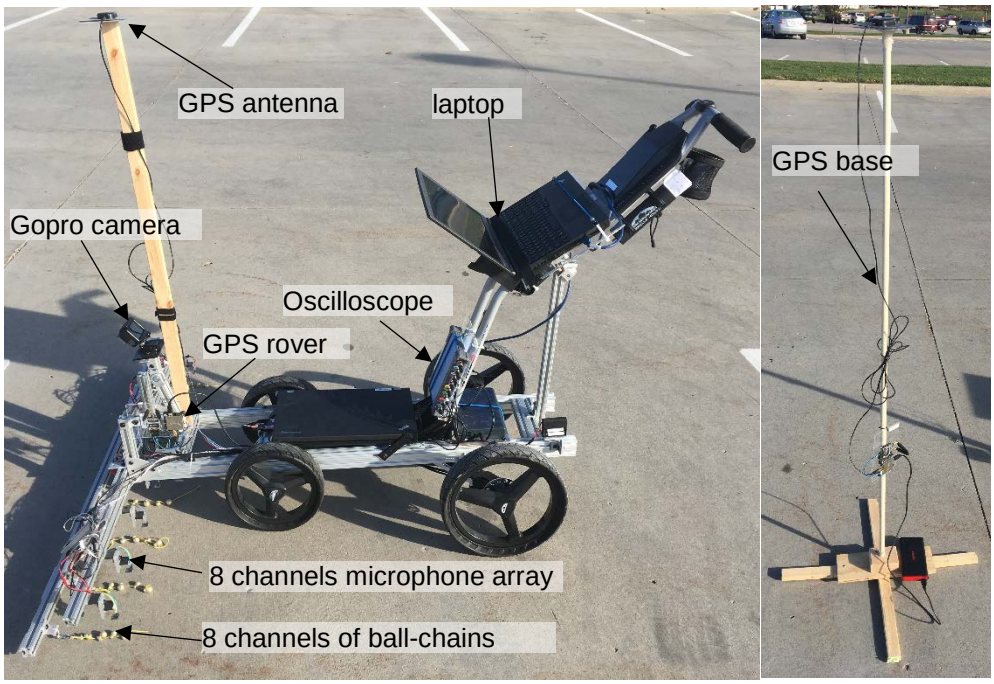

Figure 5-1 Scanning cart with RTK GPS

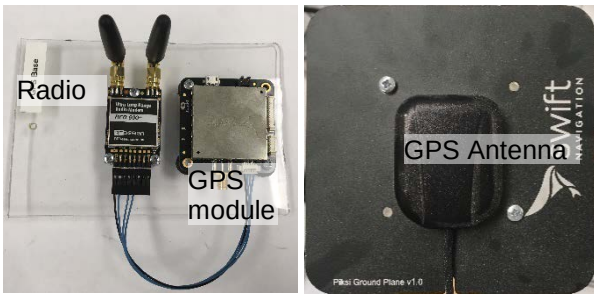

Figure 5-2 Swift RTK GPS

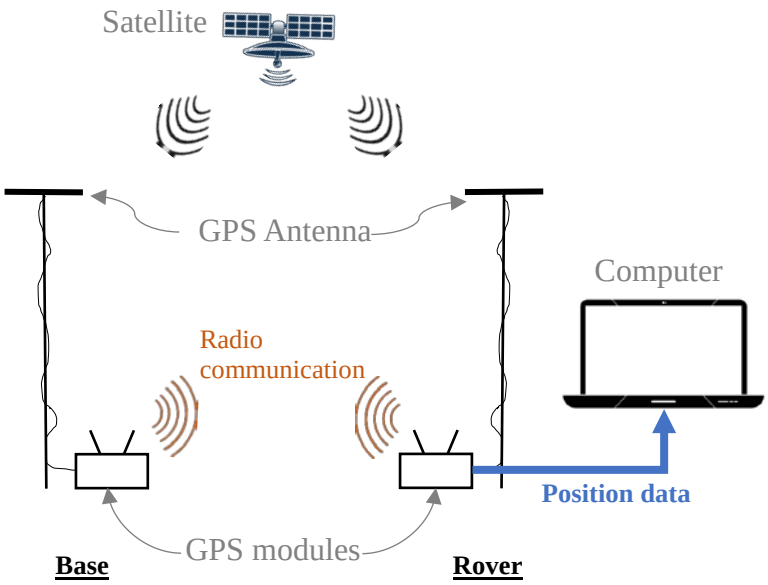

Figure 5-3 Swift RTK GPS working diagram

Before the field test, the RTK GPS accuracy was checked at a concrete parking lot with joints in south-north and west-east directions. These joints were used as the reference for the GPS rover moving paths and plotted as grid lines in **Figure 5-4**. The base GPS was placed at the origin and the rover GPS moved from the start point along the joints, then returned to the start point in clockwise direction. The relative positions of rover GPS to the base GPS were used to plot the moving path. It was concluded that the GPS has a satisfactory accuracy for bridge scanning. The measured static accuracy was within 1cm when the rover was not moving.

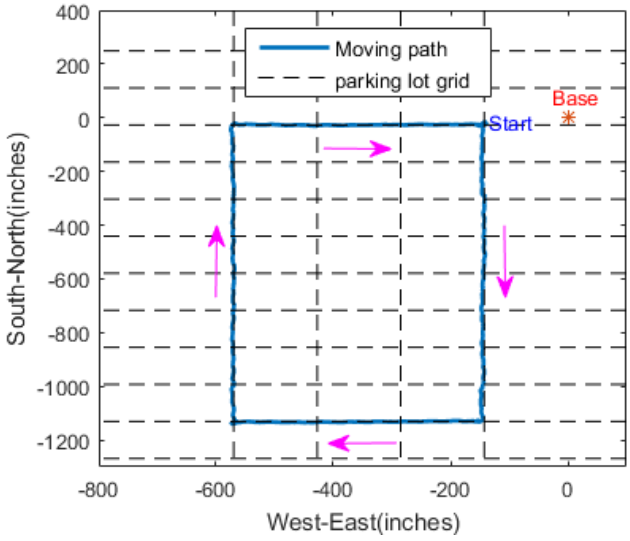

Figure 5-4 Moving path on the parking lot

A data acquisition program was designed using LabVIEW. This program has two main parts: acoustic data acquisition and real-time GPS data recording. **Figure 5-5** shows the LabVIEW data acquisition program. The acoustic signals were acquired using the LabVIEW driver of the PICO scope and the GPS data was transmitted through a Python driver embedded in the LabVIEW program. An Android application (see **Figure 5-6**) was developed based on the open source driver provided by the Swift Navigation, so that a cell phone or a tablet computer (Android system) can be used to setup the GPS base unit and record the GPS data when surveying bridge deck boundaries.

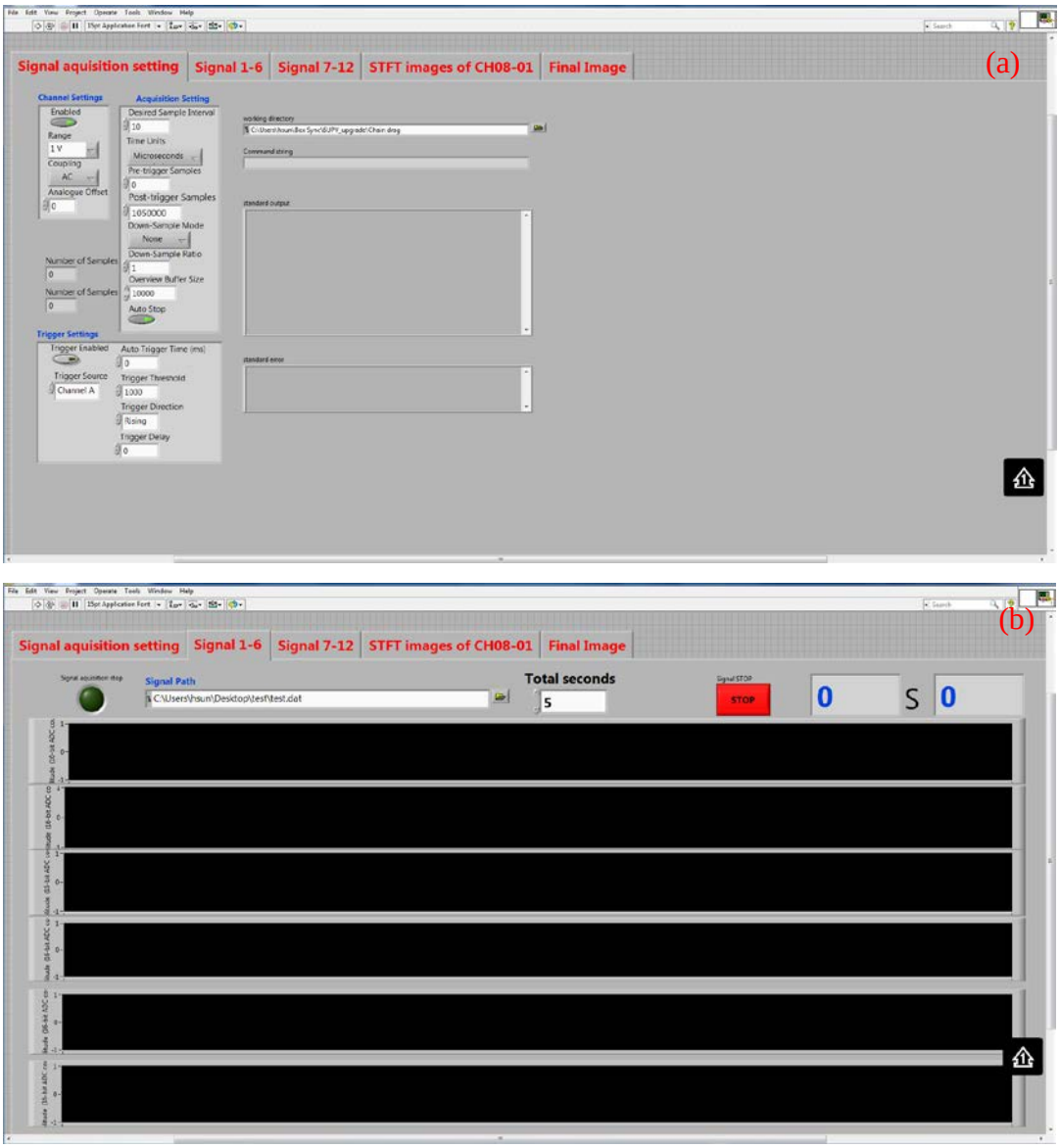

Figure 5-5 LabVIEW data acquisition program: (a) Setting page, (b) Signal display page

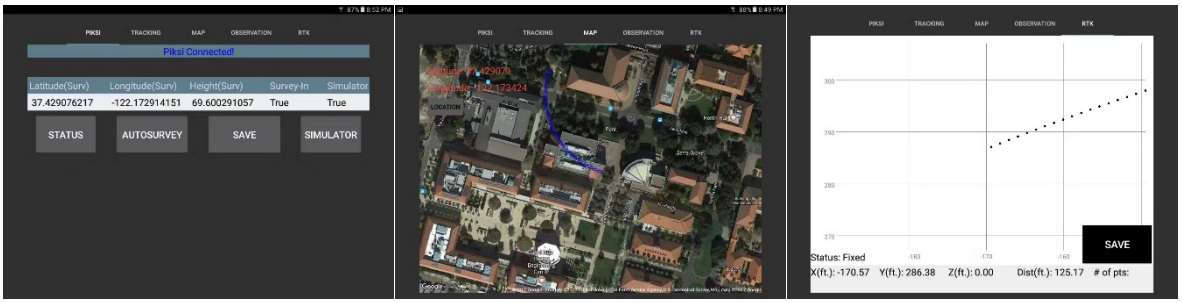

Figure 5-6 Android application for Piksi RTK GPS

5.2. Test repeatability

To investigate the repeatability of the acoustic scanning system, four scans were performed on a bridge deck (Bridge 1). Scan #1 and scan #3 were tested along the same direction and scan #2 and scan #4 were from the opposite direction. In **Figure 5-7**, a scanned area of 100 feet long by 12 feet wide with several delaminations was chosen to compare the four scanning results.

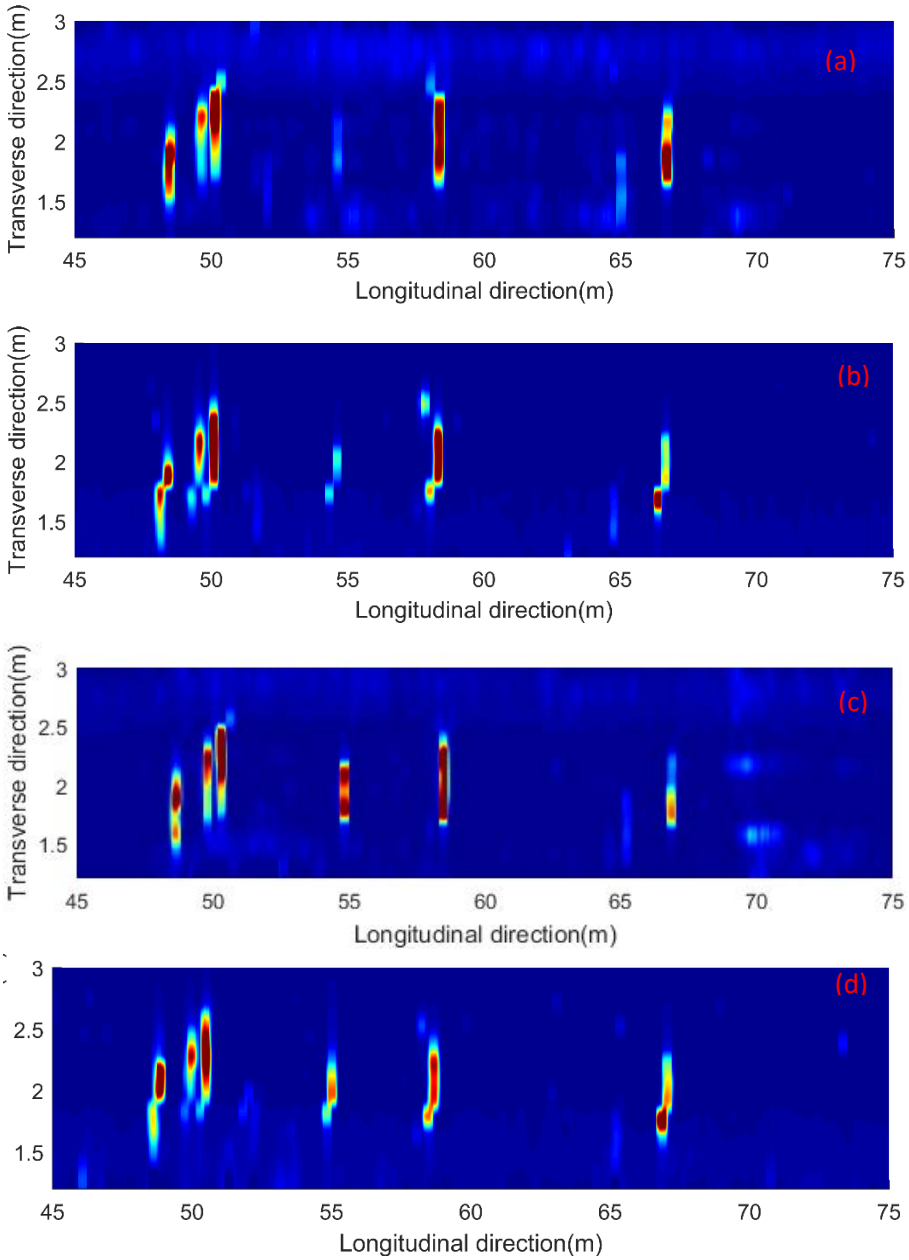

Figure 5-7 Scanning results of 30 m (100 feet) long deck: (a) scan 1, (b) scan 2, (c) scan 3, (4) scan 4

By comparing the results of four scans, we find all four images agree well with each other in terms of the locations, shapes and dimensions of all major delaminations. There are some minor differences for small size delaminations, such as the delamination near 55 m position, among the four results. Scan #3 and scan #4 clearly show this delamination with high amplitudes, while scans #1 and #2 show it with lower amplitude. In scan #2, there is a major delamination at 58 m and two small delaminations at both ends of the major delamination. These two small delaminations are also presented in scan #4 with lower amplitude. However, they are not shown in scans #1 and #3 images. The manual chain drag confirmed these two small delaminations. The results suggest scanning direction may have some effects on small delamination identification. Therefore, multiple scans from opposite directions are suggested to provide more accurate evaluation of bridge deck conditions.

5.3. Delamination identification algorithm

A delamination identification algorithm was then developed to identify the locations and dimensions of the delaminations. A two-dimensional matrix P represents the pixel amplitudes of the final scanning image. The acoustic signals in delamination areas have much higher amplitudes than in the sound areas. The algorithm can be described as the following steps:

1) The matrix P is converted to a binary matrix using threshold P_t:

$$P(i,j) = \begin{cases} 0 & if\ P(i,j) < P_t \\ 1 & if\ P(i,j) \geq P_t \end{cases} \quad (1)$$

2) Moore-Neighbor tracing algorithm modified by Jacob's stopping criteria [18] is used to trace the boundary of each possible delamination;
3) An enclosing rectangular shape boundary is generated based on the maximum length and width of the traced boundary of each delamination.
4) Location and dimensions of the delamination is determined from the rectangle.

A delamination detected in one field test is used to illustrate the boundary tracing process using the algorithm described above. In **Figure 5-8**, the red area represents a detected delamination with high signal amplitude, and the blue color represents low amplitude of background signals in sound areas. The threshold value should be determined from experience. If the image presents amplitude in linear scale, $P_t = 10\%$ of the maximum amplitude gives reasonable size of the delamination.

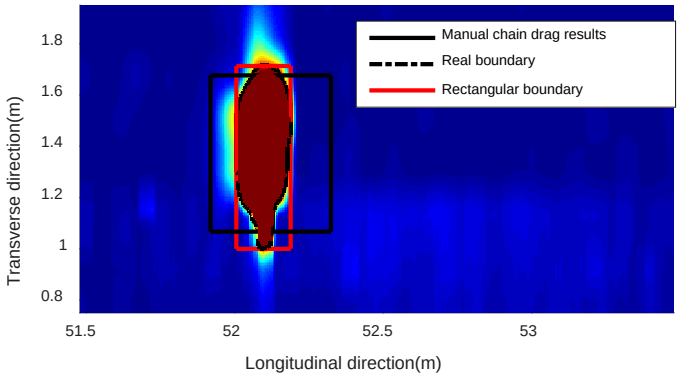

Figure 5-8 Delamination boundary tracing of Delamination #1

5.4. Field testing results

Five bridges in Omaha and Lincoln areas were tested using the automatic scanning system. The locations of the five bridges are shown in **Figure 5-9**. Detailed information of each bridge is described in Appendix B.

Figure 5-9 Locations of the five tested bridges

Figure 5-10 Google map of Bridge 1(right lane)

5.4.1. Bridge 1 (SL55W00049L, 55W southbound over railway)

This bridge is located on south bound Warlick Boulevard in Lincoln, Nebraska. The total length of the bridge is 300 feet. This bridge has been scheduled for repair during 2017-2018. This bridge was converted to two-way traffic in 2017 due to construction. The right lane was scanned in November 2016, as indicated by yellow area in **Figure 5-10**. The left lane was scanned in July 2017 shown in ***Figure 5-13***, when the left lane was used for north bound traffic.

- Right Lane

In the 2016 test, a 4-ft wide scanning frame with 8 channels was used, and therefore three runs were needed to cover the 12 feet wide lane. Each run took about 70 seconds, and a 2D image was generated after each scan. After all scans were completed, three scanning images were then combined into a full lane result. A coordinate system is built as shown in **Figure 5-10**. The *x*-axis is along the longitudinal direction (traffic direction) and *y*-axis along the transverse direction (from shoulder).

Nebraska Department of Transportation (NDOT) staff performed manual chain drag test and marked identified delaminations before the automated acoustic scanning. The size and positions of these delaminations are summarized in **Error! Not a valid bookmark self-reference.**.

Table 5-1 Positions and size of delaminations identified on right lane of Bridge 1

#	Position in long direction (feet)	Position in width direction (feet)	Width (feet)	Length (feet)
1	130.25	10.67	1.00	0.50
2	171.00	4.50	2.00	1.33
3	176.33	11.25	3.00	2.00
4	190.00	5.25	2.00	2.00
5	240.50	6.33	2.00	2.00
6	245.87	6.50	1.50	0.50

Figure 5-11 shows the acoustic scanning result of the bridge deck (right lane). In order to clearly show locations of delamination, the image is split into two parts (25-200 feet, and 200-335 feet). Before the automated acoustic scanning, manual chain drag test was performed by NDOT staff members. Five delaminations (#1, #2, #3, #5, #6) were identified and marked on the bridge deck. These delaminations are also shown in the scanning image as black rectangles. The acoustic scanning confirmed four delaminations (#1, #2, #3, #5). The positions of these four delaminations match well with the manual chain-drag results. The acoustic scanning also indicated a new delamination #4, but missed #6 in **Figure 5-11**(b). It is found #6 is a very narrow delamination. When the scanning speed is fast, about 4.5 feet/s in field testing, the ball impactors may miss very

small delaminations. Using multiple ball-chains in each channel will improve longitudinal resolution by generating more impacts than using one ball-chain. Traffic noises (circled areas) can be observed in the images, which did not affect identification of the delaminations.

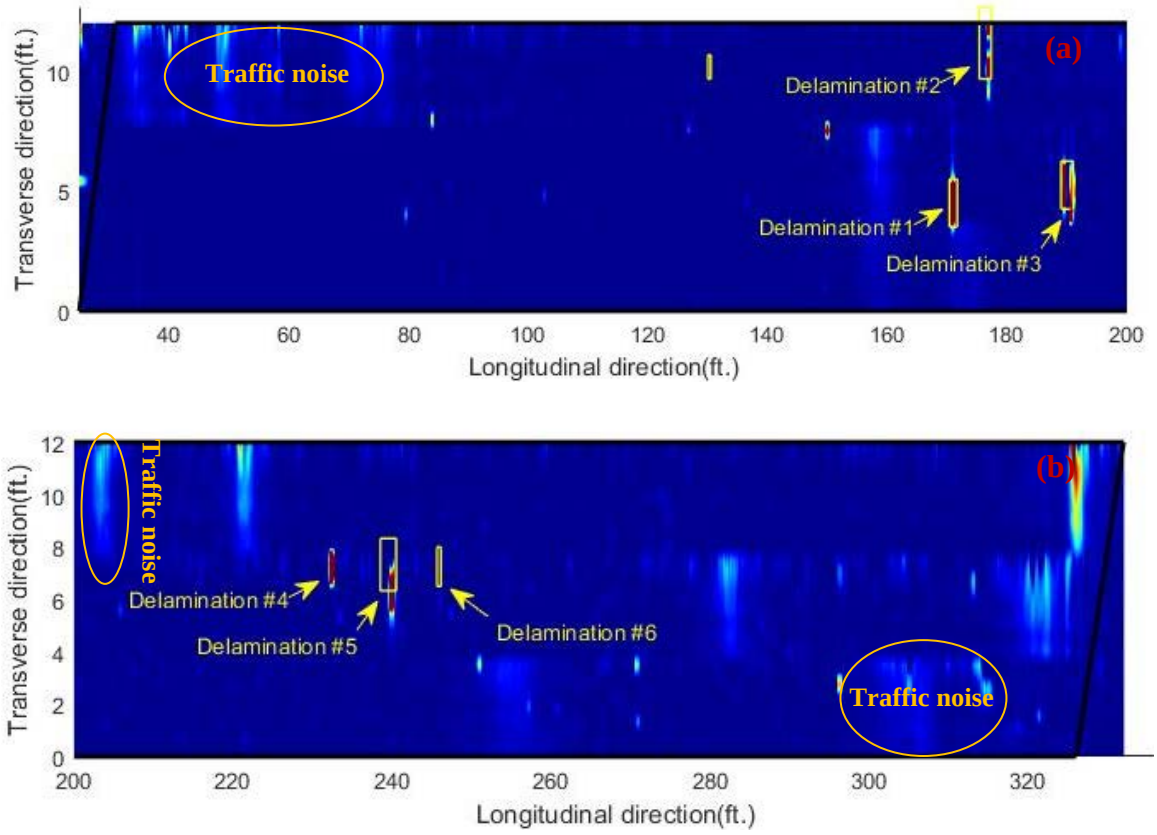

Figure 5-11 Scanning images of Bridge 1 (right lane): (a) 25-200 ft, (b) 200-335 ft

Visual inspection indicated that most detected delaminations are located around lateral surface breaking cracks or popups.

Figure 5-12 Surface cracks and marked delaminations on Bridge 1.

- Left Lane

The left lane of bridge 1 was tested in the 2017 as indicated by the yellow area in ***Figure 5-13***(a). A 6-ft wide frame with 12 channels was used for automated acoustic scanning. After the scanning, manual chain drag test was conducted to mark the positions of the delaminations. The manual chain drag results will be used as the verification of the acoustic scanning results.

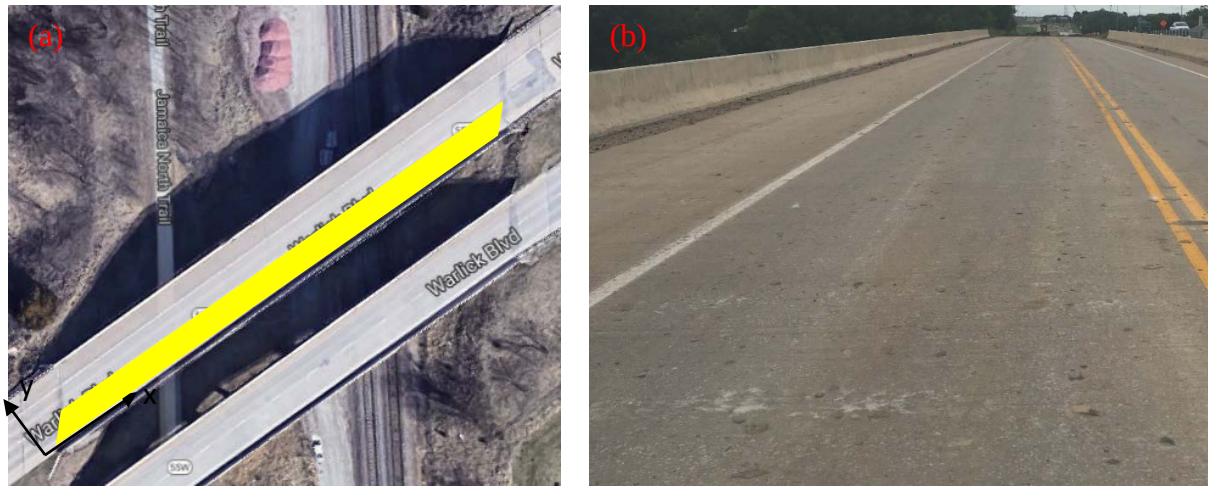

Figure 5-13 Bridge 1 (left lane): (a) Google map and the scanned area in 2017, (b) Deck surface conditions

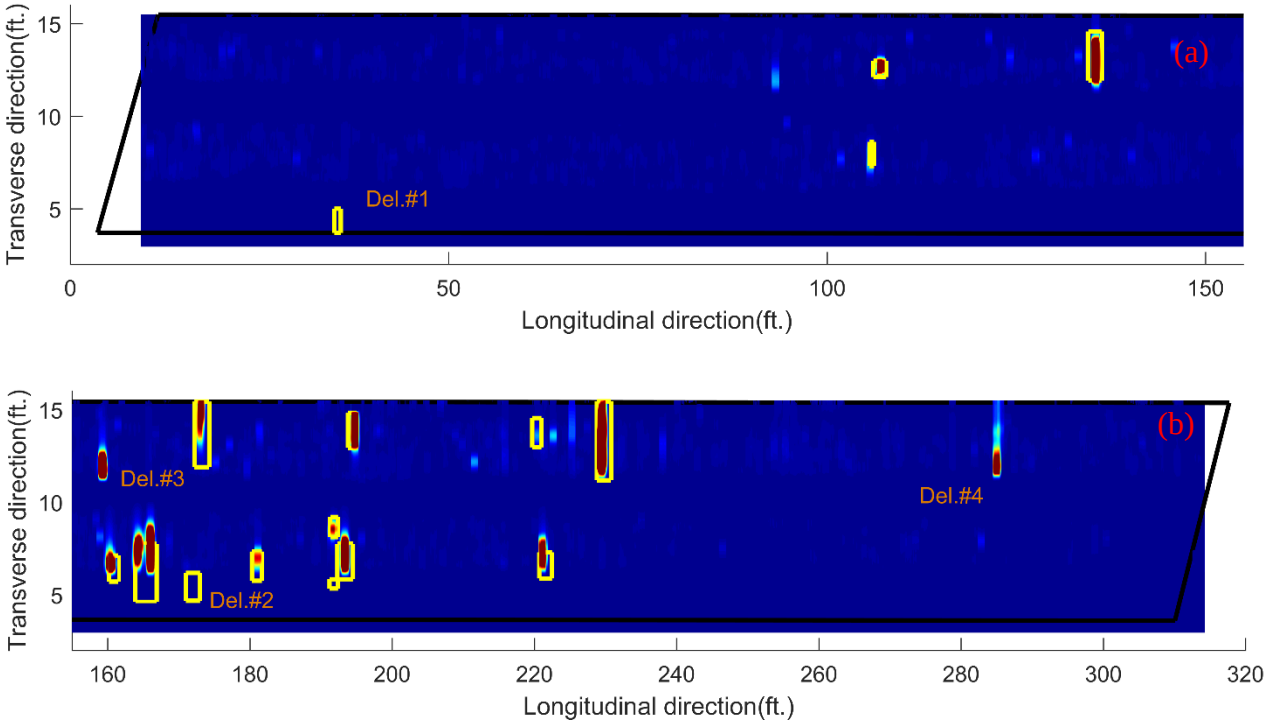

Figure 5-14 Scanning images of Bridge 1 (left lane): (a) 0-155 ft, (b) 155 ft-315 feet

Figure 5-14 shows the scanning images of the left lane of bridge deck. The image is split into two parts (0-155 ft and 155 – 315 ft). In the images, the black lines represent the bridge lane boundaries. Red spots indicate the delaminations in the bridge deck and the blue areas represent the sound deck areas. The positions of delaminations identified by the automated acoustic scanning match very well with the manual chain drag results, which are shown in yellow rectangles in the two images. However, the acoustic scanning results missed two delaminations (Del. #1 and Del. #2) which were identified by the manual chain drag. On the other hand, the acoustic scanning found two delaminations (Del. #3 and Del. #4) that were missed by the manual chain drag. Multiple scanning on the same lane confirmed these two delaminations. The total delamination area identified by the boundary tracing algorithm is about 48.1 ft^2. Compared with the scanned area 3824.4 ft^2 the delamination area percent is about 1.26 %.

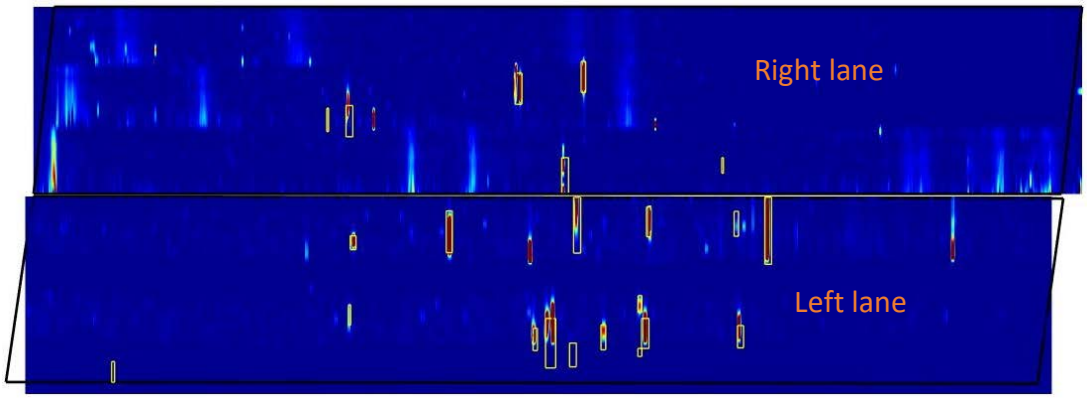

Figure 5-15 Scanning images of the two lanes on Bridge 1 (0-320 ft)

The results of the two lanes are combined in **Figure 5-15** using the same coordinate system in **Figure 5-13**. The left lane shows more delaminations than the right lane. This is probably because the left lane experience higher traffic volume than the right lane.

5.4.2. Bridge 2 (S092 46635, Hyw 92 & 240th Street, Omaha, NE)

Bridge 2 is located at Hwy. 92 & 240th Street, West Omaha. It has a concrete deck with an asphalt overlay. The overlay was removed before the deck repair in July 2017. The concrete deck had a very rough surface after the old asphalt layer was removed. The automated acoustic scanning system was then used to scan the bare concrete deck after asphalt removal. Manual chain drag test was performed by an NDOT engineer. Only the westbound lane and the shoulder (yellow area in **Figure 5-16** (a)) were tested, while the east bound lane was still open to traffic. A coordinate system is as shown in the figure below. The *x*-axis is along the longitudinal direction (traffic direction) and the *y*-axis along the transverse direction. **Figure 5-16** (b) shows the deck surface conditions after asphalt removal.

Figure 5-16 Bridge 2: (a) Google map and the scanned area, (b) Concrete deck after asphalt removal

Figure 5-17 shows the delamination map of the concrete deck. The red areas represent the delaminations and the white rectangles are these delaminations boundaries traced using the boundary tracing algorithm described before. These rectangles are used to determine the center position and sizes of the delaminations. In this scanning image, 23 delaminations are identified and the total delamination area is 196.8 feet^2 (scanned area is 684 feet^2). The delamination area percentage is defined as the ratio between delamination area and the total area, which is a critical factor for maintenance decision making. For this bridge deck, the delamination percentage is about 28.7%. However, the actual repaired area should be amplified by a coefficient about 1.5 in practice to cover small gaps between adjacent delamination areas. The details of all identified delaminations are summarized in the table below. The purple lines represent the boundary of manual chain drag results. Overall, the acoustic scanning results match well with the manual chain drag results.

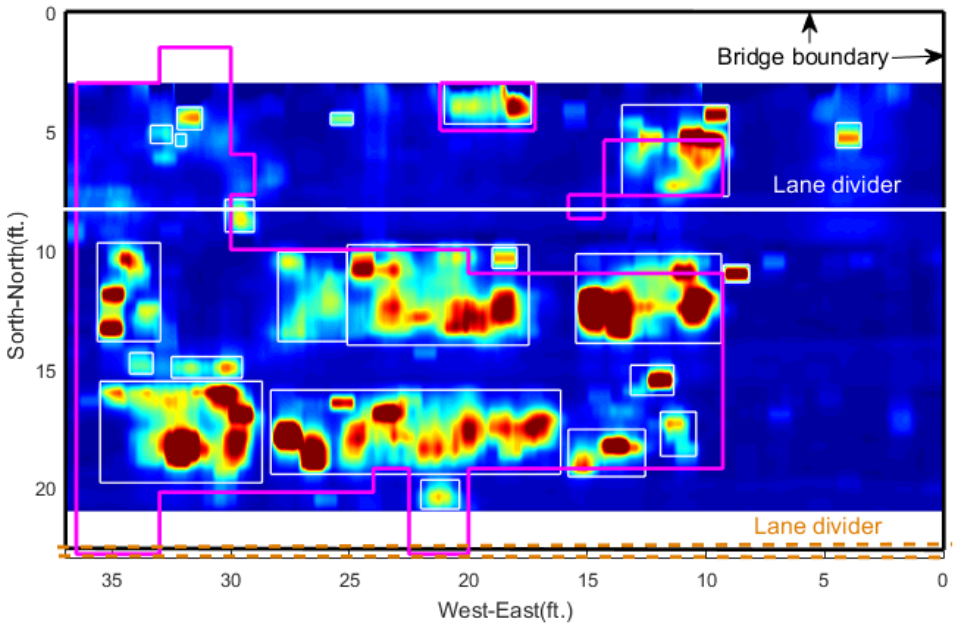

Figure 5-17 Scanning image of Bridge 2 (overlapped with manual chain drag results)

Table 5-2 Positions and size of delaminations identified on Bridge 2

#	X_{Center} (feet)	Y_{Center} (feet)	Width (feet)	Length (feet)	Area (feet^2)
1	4.01	5.2	1.06	1.04	1.10
2	8.72	11.01	1.08	0.74	0.80
3	12.42	12.06	6.12	3.76	23.01
4	11.17	17.75	1.5	1.86	2.79
5	12.27	15.49	1.82	1.26	2.29
6	14.18	18.55	3.24	1.98	6.42
7	19.19	3.86	3.66	1.72	6.30
8	21.19	20.29	1.62	1.22	1.98
9	25.33	4.51	0.94	0.5	0.47
10	32.09	17.67	6.82	4.26	29.05
11	29.63	8.58	1.22	1.36	1.66
12	31.01	14.95	2.98	0.9	2.68
13	31.73	4.49	1.06	0.94	1.00
14	32.81	6.07	0.74	0.46	0.34
15	32.92	5.16	0.92	0.76	0.70
16	33.77	14.78	0.98	0.88	0.86
17	37.4	20.42	0.64	0.68	0.44
18	37.73	5.23	0.54	0.54	0.29
19	11.29	5.84	4.5	3.84	17.28
20	22.22	17.67	12.2	3.54	43.19
21	21.28	11.91	7.64	4.22	32.24
22	26.57	11.98	2.9	3.76	10.90
23	34.29	11.79	2.66	4.14	11.01
Total area (feet^2)					196.80

5.4.3. Bridge 3 (S080 45308, Hwy 75 NB and I-80 WB intersection)

The highway intersection bridge is about 1600 feet long. We scanned three segments using the automated acoustic system, as highlighted in **Figure 5-18**. Each segment is about 300 feet long. Visual inspection indicated deteriorating surface conditions (see **Figure 5-19**) for the three segments. A quick screening scan of this area did not show any delaminations in the area between segment 1 and segment 2. Therefore, we decided to only test the three segments showing clear surface deteriorations.

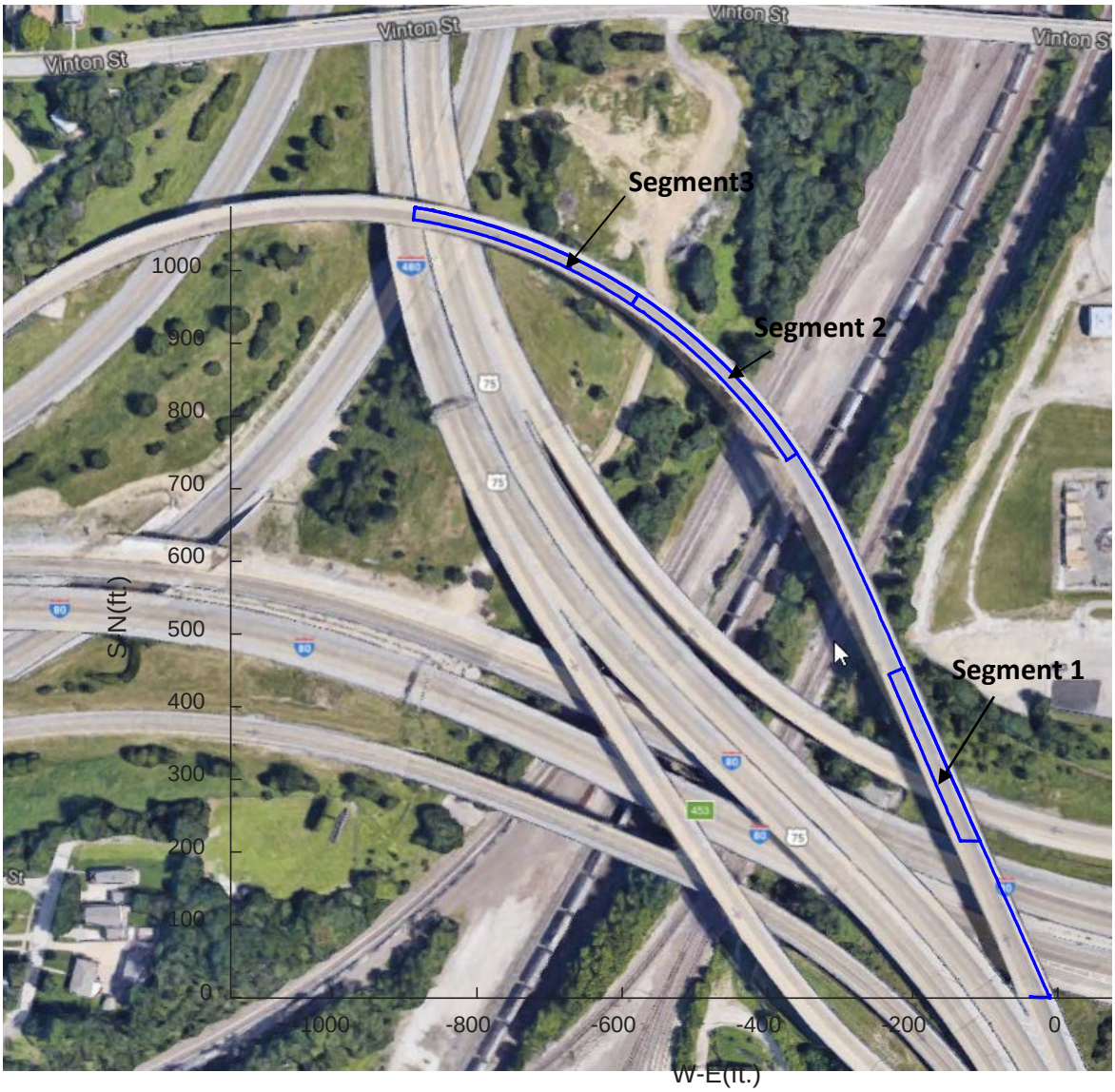

Figure 5-18 Google map of Bridge 3 and the positions of the three segments

Figure 5-19 Surface conditions of Bridge 3

In segment 1 (see **Figure 5-20**), the acoustic scanning only showed some isolated delaminations. The circled area showed more delaminations than other regions. The overall deck condition of this segment is better than segment 2 and segment 3. Acoustic scans for segment 2 (**Figure 5-21**) and segment 3 (**Figure 5-22**) showed severe delaminated areas (red areas). Delamination area and percentage for each section is summarized in **Table 5-3**.

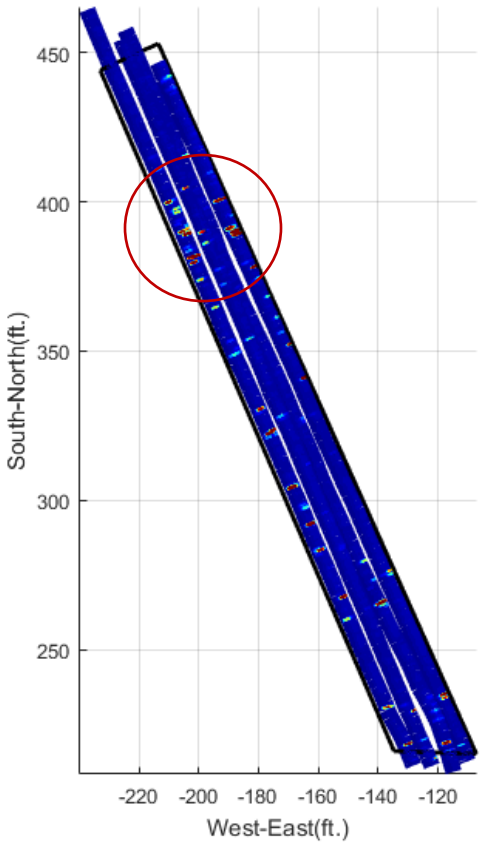

Figure 5-20 Acoustic scanning image of *segment 1* on Bridge 3

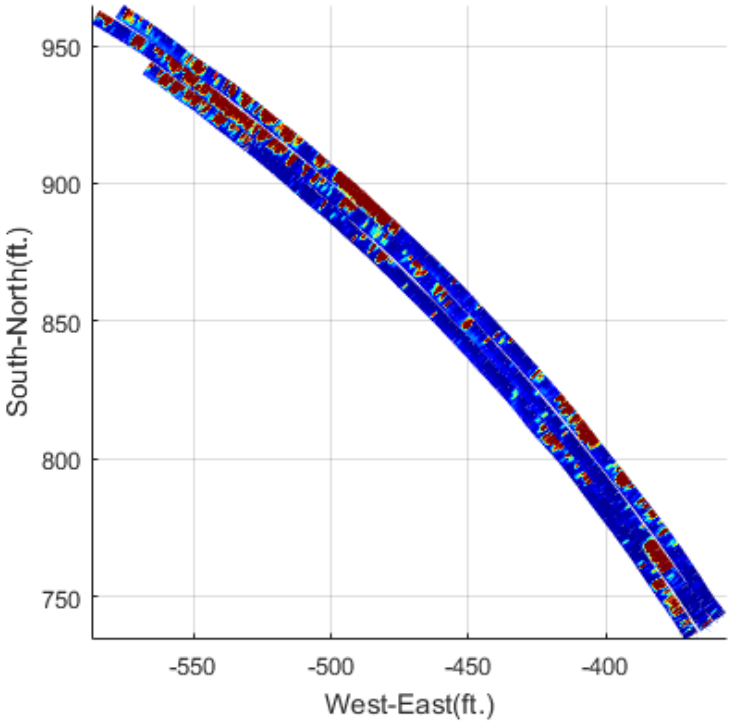

Figure 5-21 Acoustic scanning image of *segment 2* on Bridge 3

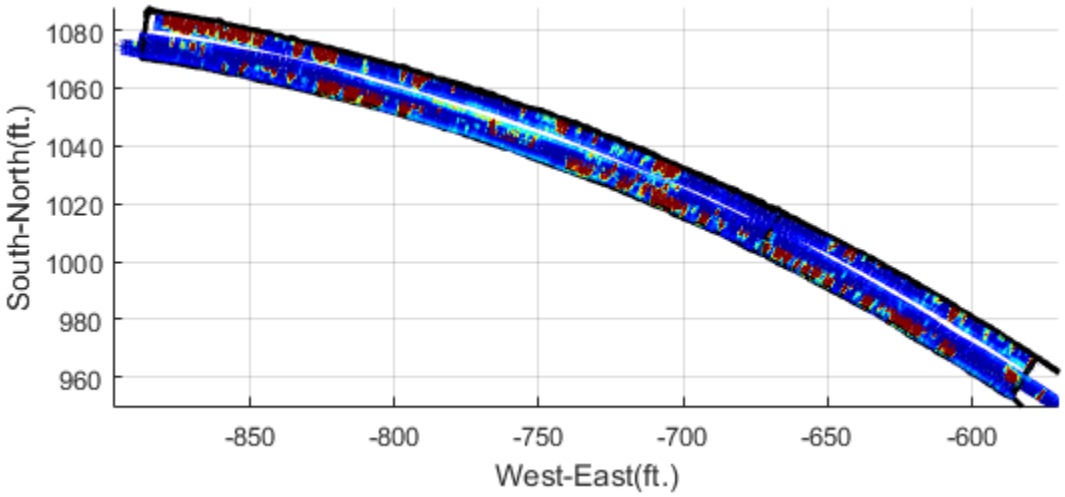

Figure 5-22 Acoustic scanning image of *segment 3* on Bridge 3

5.4.4. Bridge 4 (S080 45297, I-80 WB to I-480 NB)

The intersection bridge connects west bound highway I-80 to north bound I-480 in Omaha, NE. This bridge is about 800 feet long. One segment of 420 feet long was tested using the acoustic scanning system, as shown in **Figure 5-23**(a). Visual inspection showed severe surface deterioration (see **Figure 5-23**(b)), including many spalls and popouts.

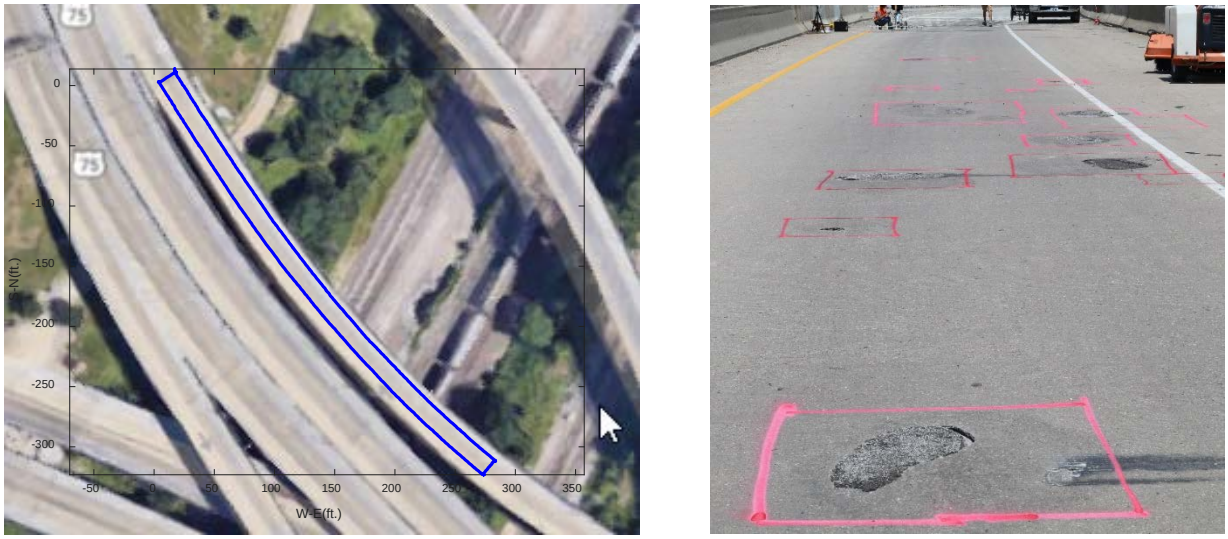

Figure 5-23 Bridge 4: (a) Google map and the scanned segment, (b) Deck surface condition

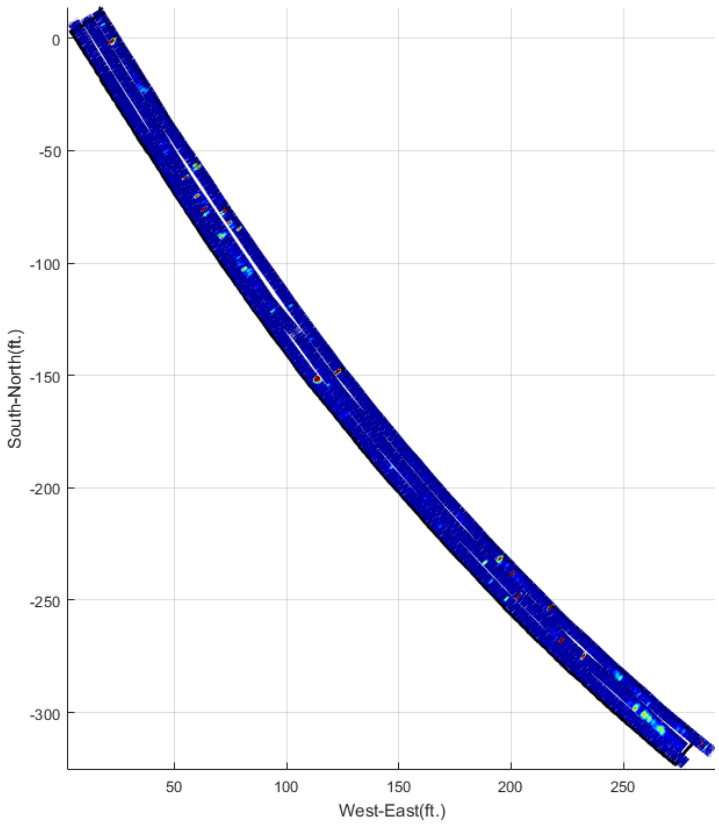

Figure 5-24 Scanning image of on Bridge 4

However, the acoustic scanning results in **Figure 5-24** showed that the deck condition was not as severe as indicated by the visual inspection. Only some isolated delaminations were identified. It seems that the acoustic scanning system did not detect the visible spalls. Therefore, the acoustic scanning should be combined with visual inspection to provide accurate and reliable evaluation.

The delamination areas and percentage for bridge 3 and bridge 4 are summarized in **Table 5-3**.

Table 5-3 Delamination area and percentage of bridge 3 and bridge 4

Bridge - segment	Scanned Area (sq ft)	Delamination Area (sq ft)	Delamination Percentage
3-1	6415.1	146.1	2.3%
3-2	5447.4	1581.2	29.0%
3-3	5415	1708.8	31.6%
Bridge 4	7489	293.7	3.9%

5.4.5. Bridge 5 (SL55W00034L, 55W southbound over creek)

Bridge 5 is located at 55W southwestern bound over Salt creek, Lincoln, NE (see **Figure 5-25**). This two lanes bridge is a 200 feet long with concrete deck. Two driving lanes and the outside shoulder were tested. A coordinate system is built as shown in the figure below. The *x*-axis is along the longitudinal direction and *y*-axis along the transverse direction.

Figure 5-25 Google map of Bridge 5

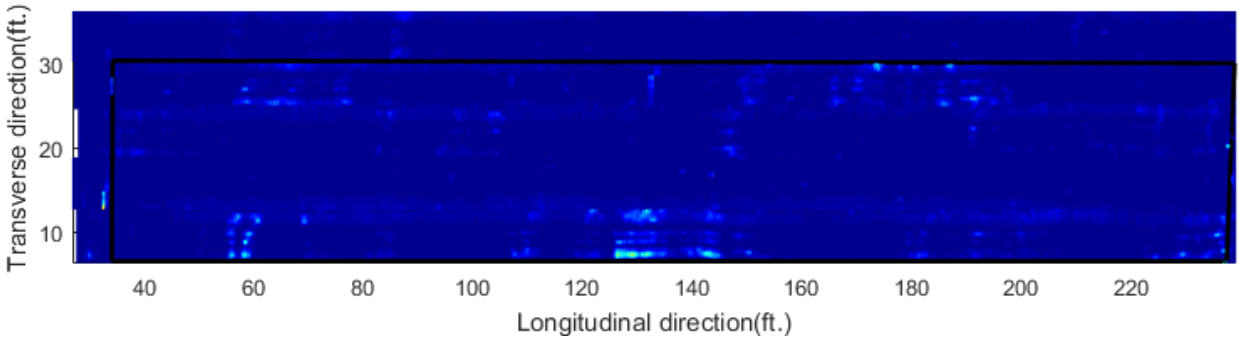

Figure 5-26 Scanning image of Bridge 5

The acoustic scanning result is shown in **Figure 5-26**. The image does not show any delaminations. Overall this bridge deck is in very good condition.

6. Conclusions

An automated acoustic scanning system was developed and implemented in bridge testing. Compared to other acoustic based scanning systems discussed in the literature review, the system developed in this study has the following advantages:

- Simple and effective source for continuous acoustic scanning
- Low cost MEMs microphones
- Multiple channel sensing with 6 inches lateral spatial resolution
- RTK GPS for high accuracy real time positioning
- Robust signal processing algorithm for imaging and mapping of delaminations

The ball-chain source is shown as a very effective acoustic source for bridge deck evaluation. It has the advantage of continuous excitation as in the chain drag test, but it provides much cleaner signals, higher signal-noise ratio, and improved repeatability than using the conventional link chains. Based on laboratory and field testing results, the following conclusions are drawn:

1. The developed ball-chain has higher S/N than the conventional steel link-chain due to the ball-chain's impact mechanism. Time domain signals generated by the ball-chain on concrete surface shows that the ball excitations are similar to the steel ball impact source used in impact-echo test. Slow motion videos showed that the balls impact the concrete surface, while the link-chain slid on surface instead, which makes the ball-chain less sensitive to surface roughness.
2. MEMs microphones are effective the acoustic sensor for delamination detection due to their high sensitivity, low cost ($1~5 each), ease of use (analog output, DC power supply). The microphone used in this study has high sensitivity and might be overload if the acoustic source is too powerful or too close to the microphone. In this study the microphone's range is suitable with the dragging ball-chain as acoustic source and the suggested distance between MEMs and ball-chain is about 2 inches (50 mm).
3. RTK GPS is a relatively new approach used on civil infrastructures and provides high precision positioning data (1cm accuracy), which can be synchronized with acoustic signals to provide real time test positions. However, the GPS only works well in open space with clear sky. It might be a concern when used in city and underneath other bridges.
4. The results of automated scanning on bridge deck agree well with manual chain drag. The automated system may miss small delaminations if no ball impacts on the delamination. This problem can be addressed by decreasing test speed or increase the number of ball impactors to improve spatial resolution in scanning direction. Preliminary study suggests a normal walking speed about 1 m/s provides satisfactory results. Using multiple balls connect in parallel may also improve the spatial resolution.
5. Multichannel interference exists between adjacent channels which will cause misjudgment of the delaminations length in the transverse direction. Further work is needed to develop separation techniques between chains/sensors. The traffic noises are not problem in this study since their levels are only about 1/10 of the delamination responses.

References

[1] ASTM D4580, “Standard Practice for Measuring Delaminations in Concrete Bridge Decks by Sounding,” West Conshohocken, PA, 2012.

[2] ASTM D6087-08(2015)e1, “Standard Test Method for Evaluating Asphalt-Covered Concrete Bridge Decks Using Ground Penetrating Radar,” West Conshohocken, PA, 2015.

[3] ASTM D4788, “Standard Test Method for Detecting Delaminations in Bridge Decks Using Infrared Thermography,” West Conshohocken, PA, 2013.

[4] M. R. Clark, D. M. McCann, and M. C. Forde, “Application of infrared thermography to the non-destructive testing of concrete and masonry bridges,” *NDT E Int.*, vol. 36, no. 4, pp. 265–275, Jun. 2003.

[5] C. L. Barnes, J.-F. Trottier, and D. Forgeron, “Improved concrete bridge deck evaluation using GPR by accounting for signal depth–amplitude effects,” *NDT E Int.*, vol. 41, no. 6, pp. 427–433, Sep. 2008.

[6] K. R. Maser, “Integration of Ground Penetrating Radar and Infrared Thermography for Bridge Deck Condition Evaluation,” *Non-Destructive Test. Civ. Eng.*, no. 2, pp. 1–8, 2009.

[7] C. Cheng and M. Sansalone, “The impact-echo response of concrete plates containing delaminations: numerical, experimental and field studies,” *Mater. Struct.*, vol. 26, no. 5, pp. 274–285, 1993.

[8] M. J. Sansalone and W. B. Streett, *Impact-echo. Nondestructive evaluation of concrete and masonry*. Bullbrier Press, Jersey Shore, PA, 1997.

[9] J. Zhu and J. S. Popovics, “Imaging Concrete Structures Using Air-Coupled Impact-Echo,” *Journal of Engineering Mechanics*, vol. 133, no. 6. pp. 628–640, 2007.

[10] S.-H. Kee, T. Oh, J. S. Popovics, R. W. Arndt, and J. Zhu, “Nondestructive bridge deck testing with air-coupled impact-echo and infrared thermography,” *J. Bridg. Eng.*, vol. 17, no. 6, 2012.

[11] T. Oh, S. Kee, R. W. Arndt, J. S. Popovics, and J. Zhu, “Comparison of NDT Methods for Assessment of a Concrete Bridge Deck,” *J. Eng. Mech.*, vol. 139, no. 3, pp. 305–314, Mar. 2013.

[12] J. S. Popovics, “Investigation of a full-lane acoustic scanning method for bridge deck,” IDEA program final report. Washington, D, C: IDEA Program, Transportation Research Board, 2010.

[13] G. Zhang, R. S. Harichandran, and P. Ramuhalli, “An automatic impact-based

delamination detection system for concrete bridge decks," *NDT E Int.*, vol. 45, no. 1, pp. 120–127, 2012.

[14] B. A. Mazzeo, J. Larsen, J. McElderry, and W. S. Guthrie, "Rapid multichannel impact-echo scanning of concrete bridge decks from a continuously moving platform," in *AIP Conference Proceedings*, 2017, vol. 1806, p. 80003.

[15] R. D. Costley and G. M. Boudreaux, "Finding delaminations in concrete bridge decks," in *146th ASA Meeting*, 2003.

[16] R. D. Costley, M. E. Henderson, and G. N. Dion, "Acoustic inspection of structures," United States patent US 6581466 B1, 2003.

[17] S.-H. Kee and N. Gucunski, "Interpretation of Flexural Vibration Modes from Impact-Echo Testing," *J. Infrastruct. Syst.*, vol. 22, no. 3, p. 4016009, Sep. 2016.

[18] R. C. Gonzalez, R. E. Woods, and S. L. Eddins, *Digital image using Matlab processing*. Person Prentice Hall, Lexington, 2003.

[19] H. Sun, J. Zhu, and S. Ham, "Acoustic evaluation of concrete delaminations using ball-chain impact excitation," *J. Acoust. Soc. Am.*, vol. 141, no. 5, p. EL477-EL481, 2017.

Appendix A: Datasheets for MEMS microphone

PRODUCT DATA SHEET

KNOWLES

SPW2430HR5H-B

1. ABSOLUTE MAXIMUM RATINGS

Parameter	Absolute Maximum Rating	Units
V_{DD} to Ground	-0.5, +5.0	V
OUT to Ground	-0.3, V_{DD} + 0.3	V
Input Current to Any Pin	±5	mA
Temperature Range	-40 to +100	°C

Stresses exceeding these "Absolute Maximum Ratings" may cause permanent damage to the device. These are stress ratings only. Functional operation at these or any other conditions beyond those indicated under "Acoustic & Electrical Specifications" is not implied. Exposure beyond those indicated under "Acoustic & Electrical Specifications" for extended periods may affect device reliability.

2. ACOUSTIC & ELECTRICAL SPECIFICATIONS

TEST CONDITIONS: 23 ±2°C, 55±20% R.H., V_{DD}(min) < V_{DD} < V_{DD}(max), no load, unless otherwise indicated

Parameter	Symbol	Conditions	Min	Typ	Max	Units
Supply Voltage[1]	V_{DD}		1.5	-	3.6	V
Supply Current[1]	I_{DD}	V_{DD} = 1.8V	-	70	95	µA
Supply Current[1]	I_{DD}	V_{DD} = 3.6V	-	75	110	µA
Sensitivity[1]	S	94 dB SPL @ 1 kHz	-45	-42	-39	dBV/Pa
Signal to Noise Ratio	SNR	94dB SPL @ 1 kHz, A-weighted (20-10kHz)	-	59	-	dB(A)
Total Harmonic Distortion	THD	94 dB SPL @ 1 kHz, S = Typ, R_{load} > 3 kΩ	-	0.1	0.2	%
Acoustic Overload Point	AOP	10% THD @ 1 kHz, S = Typ, V_{DD} = 3.6V, R_{load} > 3 kΩ	127	129	-	dB SPL
Power Supply Rejection Ratio	PSRR	200mVpp sinewave @ 1 kHz, V_{DD} = 1.8V	-	60	-	dB
Power Supply Rejection	PSR	100 mVpp square wave @ 217 Hz, V_{DD} = 1.8V, A-weighted	-	-90	-	dBV(A)
DC Output		V_{DD} = 1.5V	-	0.66	-	V
Output Impedance	Z_{OUT}	@ 1 kHz	-	-	450	Ω
Directivity			Omnidirectional			
Polarity		Increasing sound pressure	Decreasing output voltage			

[1] 100% tested.

3. FREQUENCY RESPONSE CURVE

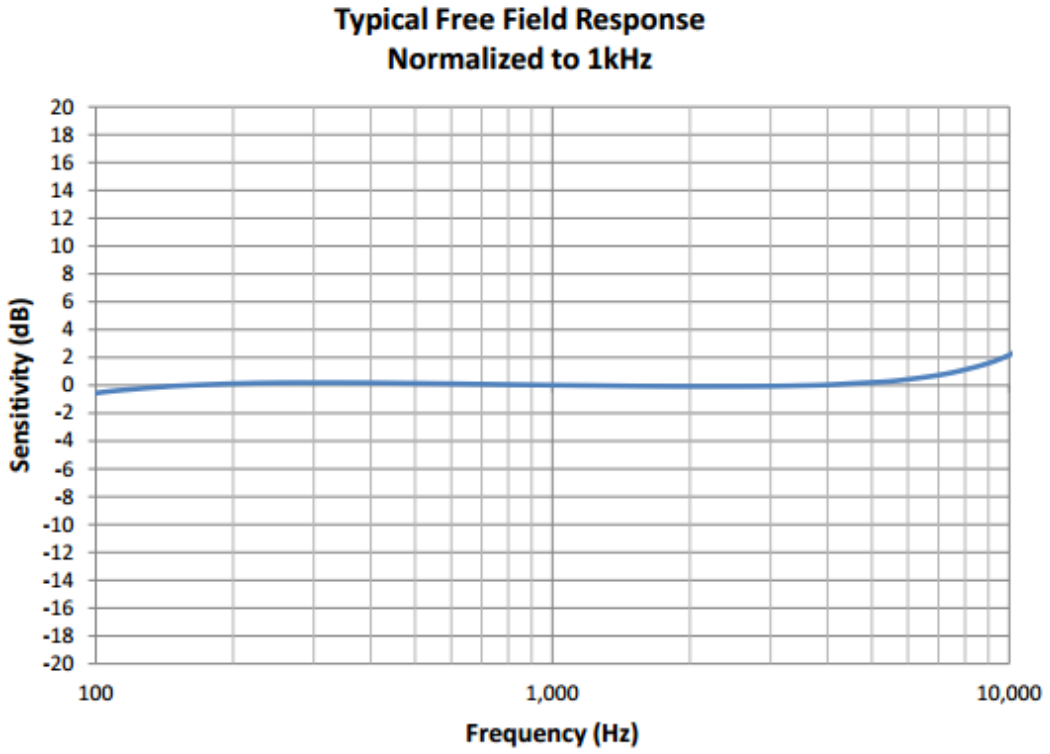

Appendix B: Bridges information

Bridge 1

Bridge 1 is located on the southwest bound of Warlick Blvd over the railway in south Lincoln Nebraska. The right lane was tested in November 2016, and the left lane was tested in July 2017.

Bridge No.	Length (feet)	Deck	Number of Lanes	Test date
SL55W00049L	300	concrete	2	11/15/2016 (right lane) 7/28/2017 (left lane)

Bridge 2

Bridge 2 is located at the cross of US Highway 92 and US Highway 275 in west Omaha NE. Only the westbound lane was tested.

Bridge No.	Length (feet)	Deck information	Number of Lanes	Test date
S09246635	36	Concrete with asphalt overlay	1	06/26/2017

Bridge 3

Bridge 3 is the intersect bridge of US Highway 75 northbound to I80 westbound. Three segments of this bridge were tested.

Bridge No.	Length (feet)	Deck information	Number of Lanes	Test date
S08045308	1600	concrete	2	07/06/2017

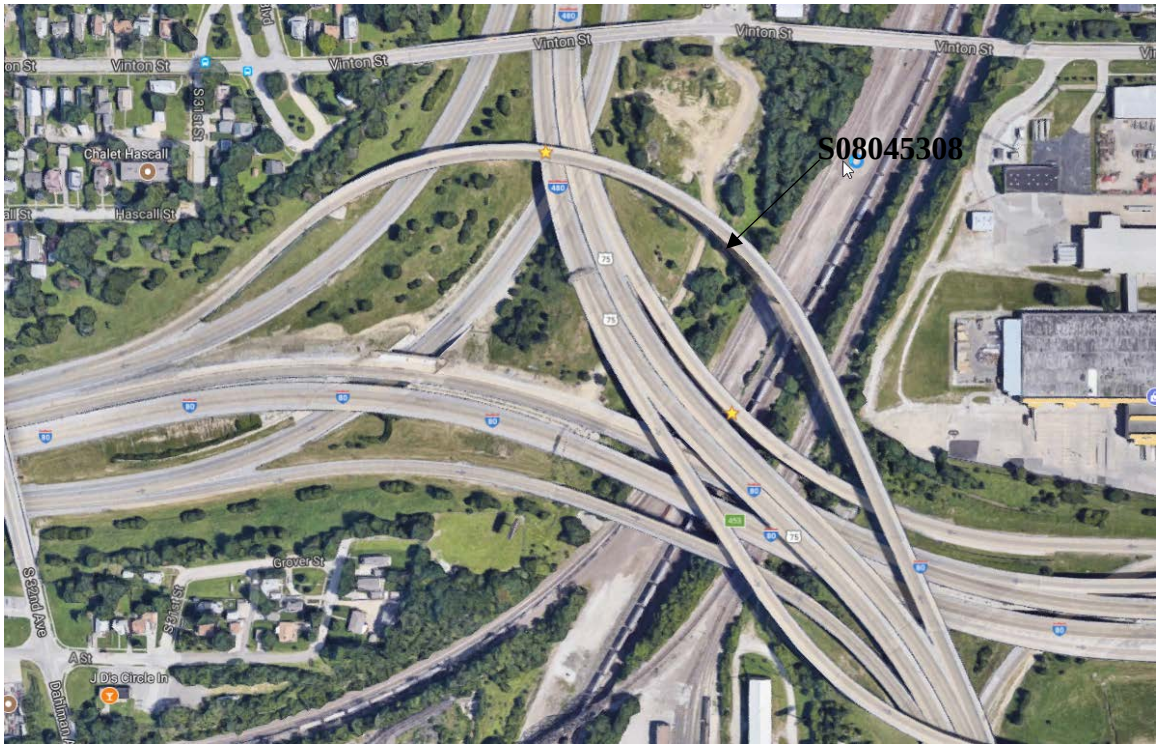

Bridge 4

Bridge 4 is the ramp bridge of I80 westbound to 480 northbound. One segments of this bridge were tested.

Bridge No.	Length (feet)	Deck information	Number of Lanes	Test date
S08045297	600	concrete	1	07/06/2017

Bridge 5

Bridge 5 is located on the southwest bound of Warlick Blvd over Salt creek in south Lincoln Nebraska. All lanes are tested.

Bridge No.	Length (feet)	Deck information	Number of Lanes	Test date
SL55W00034L	260	concrete	2	07/28/2017